

AUTOMATED 3D SOLID FEM GENERATOR OF COMPLEX STRUCTURES
USING LASER SCAN DATA

A THESIS SUBMITTED TO
THE GRADUATE SCHOOL OF NATURAL AND APPLIED SCIENCES
OF
MIDDLE EAST TECHNICAL UNIVERSITY

BY

MAHA O. M. SHAREI

IN PARTIAL FULFILLMENT OF THE REQUIREMENTS
FOR
THE DEGREE OF MASTER OF SCIENCE
IN
CIVIL ENGINEERING

FEBRUARY 2019

Approval of the thesis:

**AUTOMATED 3D SOLID FEM GENERATOR OF COMPLEX
STRUCTURES USING LASER SCAN DATA**

submitted by **MAHA O. M. SHAREI** in partial fulfillment of the requirements for
the degree of **Master of Science in Civil Engineering Department, Middle East
Technical University** by,

Prof. Dr. Halil Kalıpçılar
Dean, Graduate School of **Natural and Applied Sciences**

Prof. Dr. Ahmet Türer
Head of Department, **Civil Engineering**

Prof. Dr. Ahmet Türer
Supervisor, **Civil Engineering, METU**

Examining Committee Members:

Prof. Dr. Özgür Kurç
Civil Engineering, METU

Prof. Dr. Ahmet Türer
Civil Engineering, METU

Prof. Dr. Murat Altuğ Erberik
Civil Engineering, METU

Assist. Prof. Dr. Onur Pekcan
Civil Engineering, METU

Assist. Prof. Dr. Halit Cenan Mertol
Civil Engineering, Atilim University

Date: 01.02.2019

I hereby declare that all information in this document has been obtained and presented in accordance with academic rules and ethical conduct. I also declare that, as required by these rules and conduct, I have fully cited and referenced all material and results that are not original to this work.

Name, Surname: Maha O. M. Sharei

Signature:

ABSTRACT

AUTOMATED 3D SOLID FEM GENERATOR OF COMPLEX STRUCTURES USING LASER SCAN DATA

Sharei, Maha O. M.
Master of Science, Civil Engineering
Supervisor: Prof. Dr. Ahmet Türer

February 2019, 60 pages

For newly designed buildings, 3D modeling has become an integral part of analysis and design procedure using several simplified approaches by recognized and available software; in which user manually defines the geometry, loads, material properties, and support conditions of structures. Nevertheless, geometry modeling for historical complex structures, especially for masonry type construction, wall thicknesses, openings, section losses are difficult to be accurately defined in analysis programs. Changing wall thickness and alterations to the geometry of historical structures are usually difficult to be modeled with shell members. Therefore, a 3D solid FEM is more accurate for modeling of complex masonry structures.

Laser scanning cameras are now widely used for taking inside and outside architectural surveys. The available commercial 3D solid meshing tools are very sensitive to the accuracy and perfection of the volumetric geometry. The development of an innovative algorithm to directly generate 3D solid finite element model (FEM) using point cloud is targeted in this thesis. The developed algorithm is applied and tested on two case studies of complex masonry structures. A comparison of analysis results of the historical structure of Şehzade Mosque is carried out between a volumetric solid finite element model generated with the developed software and a simplified shell FEM.

The solid models that are automatically generated using the developed software have more realistic results regarding stress distribution; whereas, shell model has higher stress concentrations because of sharp edges and distortion of the geometry.

Keywords: Historical Structures, Laser Scanning, Automatic Mesh Generation, Finite Element Modeling, Structural Analysis

ÖZ

LAZER TARAMA VERİLERİ KULLANARAK OTOMATİK ÜÇ BOYUTLU KATI SONLU ELEMANLAR MODELİ OLUŞTURMA

Sharei, Maha O. M.
Yüksek Lisans, İnşaat Mühendisliği
Tez Danışmanı: Prof. Dr. Ahmet Türer

Şubat 2019, 60 sayfa

Yeni tasarlanan binalar için, 3D modelleme, tanınmış ve mevcut yazılımlar kullanılarak basitleştirilmiş birkaç yaklaşım ile analiz ve tasarım prosedürünün ayrılmaz bir parçası haline gelmiştir. Kullanıcılar manuel yöntemler kullanarak yapıların geometrisini, yükleri, malzeme özelliklerini ve mesnet koşullarını tanımlamaktadır. Bununla birlikte, tarihsel kompleks yapıların geometrik modellemesi için, özellikle duvar kalınlıklarının, duvardaki pencere kapı boşluklarının, kesit kayıplarının analiz programlarında doğru bir şekilde tanımlanması daha zordur. Duvar kalınlığının kabuk elemanları kullanılarak modelleme yapılması genellikle daha zordur; ayrıca, kabuk elemanların kalın duvarları modellemek için kullanılması oldukça yaklaşık bir modelleme tekniğidir. Bu nedenle, karmaşık duvar yapılarının modellenmesi için 3D katı sonlu elemanlar modelinin kullanılması daha doğrudur. Lazer tarama kameraları günümüzde mimari uygulamalarda içten ve dıştan yüzey tarama ve rölöve çıkarmak için yaygın olarak kullanılmaktadır. Mevcut ticari 3D katı modelleme yazılımları, lazer bulutundan elde edilen yüzey geometri doğruluğu ve mükemmelliğine karşı çok hassastır. Bu tezde, doğrudan üç boyutlu (3D) katı sonlu elemanlar modelini (FEM) üretmek için yenilikçi bir algoritmanın geliştirilmesi hedeflenmiştir. Geliştirilen algoritma, karmaşık duvar yapılarının bulunduğu iki pilot yapı çalışmasında uygulanmış ve test edilmiştir. Tarihi Şehzade

Camii'nin sonlu elemanlar analiz sonuçları yeni geliştirilen yazılımla oluşturulan hacimsel katı ve basitleştirilmiş kabuk modelleri kullanılarak karşılaştırılmıştır.

Geliştirilen yazılım kullanılarak oluşturulan katı model sonuçları daha gerçekçi gerilim dağılımı sonuçları verirken, kabuk model kullanılarak oluşturulan modellerde geometrinin bozulması ve keskin köşeler sebebiyle gerilme konsantrasyonu bölgeleri oluşmuştur.

Anahtar Kelimeler: Tarihi Yapılar, Lazer Tarama, Otomatik Ağ Oluşturma, Sonlu Elemanlar Modellemesi, Yapısal Analiz

To My Parents

ACKNOWLEDGEMENTS

I would like to express my sincerest gratitude to my advisor Prof. Dr. Ahmet Türer for his guidance, patience, time and knowledge generosity during the development of the innovative idea behind this thesis.

A special thanks go to my noble spouse Nabil Abubaker for his endless love and encouragement. I want also to thank him for his support during the programming part of this study.

I would also like to express my gratitude to my parents, brothers, sister, family in-law and all my friends for their love and support to overcome the challenge behind the completion of this thesis.

Finally, I would like to thank YÜKSEL PROJE Inc. for their financial support for Şehzade Mosque Assessment Project, and for providing laser scan data used to generate the solid FE Model of the structure.

TABLE OF CONTENTS

ABSTRACT	v
ÖZ.....	vii
ACKNOWLEDGEMENTS	x
TABLE OF CONTENTS	xi
LIST OF TABLES	xiii
LIST OF FIGURES	xiv
1. INTRODUCTION	1
1.1. Problem Statement.....	1
1.2. Literature Review	3
1.3. Objective and Scope	7
1.4. Laser Scanning and Data Pre-Processing	7
2. AUTOMATED 3D SOLID FEM GENERATOR	11
2.1. Defining Boundary Solids Using Scan Data (Mapping)	12
2.1.1. Scan Data Reading and Parameters Definition.....	12
2.1.2. Boundary Mapping with Points	15
2.1.3. Boundary Mapping Without Points	15
2.2. Defining Internal Solids.....	16
2.2.1. 2D-Navigation Approach for Internal Mesh Definition.....	16
2.2.2. 3D-Navigation Approach for Internal Mesh Definition.....	18
2.3. Finite Elements Generation.....	20
2.4. Time and Memory Efficiency Improvement	22
2.5. Finite Element Model Smoothing	23

3. GENERATOR VALIDATION: CASE STUDIES	25
3.1. A Masonry Bridge FEM Generation	25
3.2. Şehzade Mosque Modeling and Analysis	28
3.2.1. 3D-Shell Finite Element Model	29
3.2.2. 3D-Solid FE Model	32
3.2.3. Dynamic Testing and Analysis Results	38
3.2.3.1. Dynamic Test Result	38
3.2.3.2. 3D- Shell FEM Analysis	39
3.2.3.3. 3D- Solid FEM Analysis	43
3.2.3.4. Comparison Between Shell and Solid FEM Analysis Results	45
4. CONCLUSIONS AND FUTRUE WORK	53
REFERENCES	55
APPENDIX	59

LIST OF TABLES

TABLES

Table 3.1. Material properties after calibration and thickness of sections.....	40
Table 3.2. Comparison between solid models of Şehzade mosque with different mesh size	44
Table 3.3. Comparison between 3D shell and solid models for Şehzade mosque	45
Table 3.4. Number and percentage of safe and unsafe shell and solid elements of Şehzade mosque FE models	52

LIST OF FIGURES

FIGURES

Figure 1.1. Ariel view of Şehzade Mosque- Istanbul	2
Figure 1.2. Interior view of Şehzade Mosque (Islamic Arts Magazine).....	3
Figure 2.1. Hypothetical scan data	11
Figure 2.2. The boundary cubes of the dome ($\Delta=0.25$ m)	16
Figure 2.3. The distribution of zones, and starting cubes for the recursive function in an XY section of the dome	18
Figure 2.4. The distribution of zones when 3D navigation is used for the dome.....	19
Figure 2.5. The flowchart for the generator algorithm using 3D navigation for internal solids definition	20
Figure 2.6. The internal boxes of the dome ($\Delta=0.25$ m).....	21
Figure 2.7. The boundaries and internal meshes of the dome ($\Delta=0.25$ m)	22
Figure 3.1. Onaç Masonry Bridge (YAVUZ MİMARLIK, 2017).....	25
Figure 3.2. The scan data of Onaç masonry bridge	26
Figure 3.3. The clean cloud of Onaç masonry bridge.....	26
Figure 3.4. The surface mesh for Onaç masonry bridge	27
Figure 3.5. The final cloud of Onaç masonry bridge.....	27
Figure 3.6. The 3D hexahedral FE model of Onaç masonry bridge ($\Delta=0.2$ m)	28
Figure 3.7. The general view of Şehzade Mosque- Istanbul.....	29
Figure 3.8. 3D shell model of Şehzade mosque	30
Figure 3.9. Internal and external complex geometry of Şehzade mosque	30
Figure 3.10. Frames used to model spandrels and pendentives	31
Figure 3.11. Rings used to model the surrounding frames for domes	31
Figure 3.12. Rigid members for dome to wall and dome to column connections.....	32
Figure 3.13. Registration of the scans of Şehzade mosque	32
Figure 3.14. Inside and outside scans of Şehzade mosque	33

Figure 3.15. Slice 3 of inside and outside scans after cleaning	34
Figure 3.16. The slices of inside and outside scans after cleaning	34
Figure 3.17. Outside surface mesh before and after healing.....	35
Figure 3.18. The final cloud sampled from the repaired surface mesh	36
Figure 3.19. The 3D hexahedral FE model of Şehzade mosque ($\Delta=0.2$ m)	37
Figure 3.20. 1st mode frequency measured by accelerometers installed at minarets	38
Figure 3.21. Ambient vibration recorded at the main dome	39
Figure 3.22. Response spectrum function definition using Turkish code.....	40
Figure 3.23. First six modal shapes	41
Figure 3.24. Construction stages	42
Figure 3.25. Tension stresses S22 from dead and staged dead loads	42
Figure 3.26. First mode of the solid model of the mosque	43
Figure 3.27. Fifth mode shape and period of the shell model.....	43
Figure 3.28. A vertical section in solid models with 0.2, 0.3, 0.4, 0.5 m mesh size .	44
Figure 3.29. Gravity loads tension and compression stresses in the shell model.....	46
Figure 3.30. Tension stresses from DL and X-direction EQ for both models (0 - 1 MPa & 0 - 2 MPa).....	47
Figure 3.31. Tension stresses from DL and Y-direction EQ for both models (0 - 1 MPa & 0 - 2 MPa).....	48
Figure 3.32. Compression stresses from DL and X-direction EQ for both models (0 - 2 MPa).....	49
Figure 3.33. Compression stresses from DL and Y-direction EQ for both models (0 - 2 MPa).....	49
Figure 3.34. Limits of principle stresses using Coulomb-Mohr Theory.....	51
Figure 3.35. Principle stresses for shell elements compared to limits.....	51
Figure 3.36. Principle stresses for solid elements compared to limits.....	52
Figure A.1. Tension stresses from dead load and TH load in X-direction (0 - 1 & 0 - 2 MPa).....	60
Figure A.2. Compression stresses from dead load and TH load in X-direction (0 - 2 MPa).....	60

CHAPTER 1

INTRODUCTION

1.1. Problem Statement

Within the scope of historical structures preservation, Terrestrial Laser Scanners (TLS) have been widely used in documentation, Building Information Modeling (BIM), stability studies, and structural health monitoring. For instance, the Turkish government recently put an intensive effort in the documentation and restoration for Turkish cultural heritage. The laser scanning is hired for geometry preparation and structural behavior study of historical structures which facilitates the strengthening and rehabilitation process.

Laser scanning is a surveying method to accurately capture entire details of buildings. The result of a laser scanning process is a set of points with three dimensional coordinates called “point cloud” which represents the 3D shape of a building (Hayes and Richie, 2015). Hayes and Richie added that “most of as-built drawings are inaccurate and incomplete, if a building renovation or retrofit is designed based on outdated or incomplete drawings, errors will be “designed in”. Hence, laser scanning is a helpful accurate surveying method in building construction field (Hayes and Richie, 2015).

Several point cloud tools (for example CloudWorx for Revit and CloudCompare) can be used for viewing, registering, filtering and modifying scan data. Furthermore, many algorithms and software have been used for surface construction out of laser scan data. These tools have the following problems: full details of scanned objects or structures can't be captured, high level of human interaction is needed (Hinks, et al., 2012). Due to the simplifications and assumptions used in shell modeling (e.g. assumptions made to simplify elements thickness irregularity), either by using traditional CAD-based

modeling approach or surface meshing and triangulation of point clouds, the modeling and analysis of FEM of complex historical structures becomes inaccurate and time-consuming. Some recent works focused on volumetric meshing in 3D modeling (e.g. pyramids, tetrahedral or hexahedral finite elements) to better capture the geometry of complex monumental structures. However, commercial 3D solid meshing tools are very sensitive to the accuracy and perfection of the volumetric geometry (Kaszynski et al.,2018).

A semi-automatic 3D solid finite element mesh generation based on surveyed point clouds of complex historical buildings was developed by Castellazzi in 2015. The authors were able to reduce the time and labor effort needed to build FE models of complex monumental structures compared to the traditional time-consuming CAD-based process of converting TLS surveys to FE models (Castellazzi et al., 2015). However, the slicing, splitting and digitization process used in the previous mentioned literature was still considered as labor-intensive and time-consuming approach (Bitelli et al. ,2016). Therefore, a three dimensional FE modeling with volumetric meshes to automatically capture the full details of structures with complex geometry using TLS survey is discussed in this thesis. The laser scanning data for two historical structures, a masonry bridge and Şehzade mosque, are used to develop and validate the 3D-solid FEM generator. Figures 1.1 and 1.2 respectively show the inside and outside of Şehzade mosque.



Figure 1.1. Ariel view of Şehzade Mosque- Istanbul



Figure 1.2. Interior view of Şehzade Mosque (Islamic Arts Magazine)

1.2. Literature Review

Terrestrial Laser scanning (TLS) has been increasingly used in Building Information Modeling (BIM) and cultural heritage preservation studies. Laser scanners are remote tools to collect high accuracy data with high acquisition rate providing millions of measurements in three dimensions called “point clouds”.

In the context of using TLS in BIM, Huber, et al. studied a potential automatic transformation from point clouds to as-built models and focused their study to the main components of buildings, such as walls, floors and ceilings. This study was done to exempt the drawbacks and limitations of the manual, costly, time-consuming and error-prone “points-to-BIMs transformation” process (Huber, et al.,2011).

In a recent work, Korumaz, et al., (2017) discussed the main structural modeling techniques. The most popular method among them is the use of Computer Aided Design (CAD) software to build 3D models, the geometrical dimensions can be extracted by traditional manual survey or laser scanning technique. In both cases, some simplifications and corrections are made to the original geometry of buildings.

In many condition, vulnerability and restoration studies of historical structures, the 3D FE models were built with the help of laser scanners. For instance, TLS technique was

used in the assessment and maintenance of “Cernadela” masonry bridge. A solid FEM of the bridge was built in several steps. Firstly, the point cloud of the bridge was separated from surrounding data using cleaning and segmentation process, then 2D Delaunay triangulation was carried out for each wall of the bridge according to the visualization plane, texturing was applied to the surface model and the photorealistic 3D surface model was used to generate the 3D solid model using CAD-based tools (Lubowiecka, et al.,2009). Another geometrical modeling of a masonry bridge using photogrammetry survey was carried out to a “Mediaeval Bridge”. The Delaunay triangulation was performed to construct a surface mesh for the boundary points of each stone, then a set of triangles was fitted to each stone surface (Arias, et al., 2007).

Moreover, in (Korumaz, et al., 2017), a 3D FE model for a brick minaret was obtained and employed for health assessment of the structure based on Terrestrial Laser Scanning (TLS) technology. Cyclone 8.0 software was used for post-processing of the detailed point cloud of the minaret, then a 3-million-point cloud was transferred in PTX format to MeshLab software for triangulation. The surface mesh was then converted to watertight mesh to be used in FE analysis software.

Several other studies were focused on surface, shell and triangulation meshing of point clouds of scanned objects. Pauly, et al. stated that in order to get high level of details for a surveyed object using surface mesh, many geometrical processing algorithms are used for surface reconstruction from laser scan data (Pauly, et al., 2004).

A three-dimensional model for the dome of Mihrimah Sultan Mosque was generated with the help of laser scanners. Cyclone 9.1.5 software was used to register, clean and filter the acquired point cloud of the dome. Next, a 3D triangulated surface mesh was created by 3DReshaper tool. Finally, the mesh was imported to SAP2000, shell element thickness, boundary conditions and other properties were assigned to the FE model (Ercan and Cakti, 2017).

Barrille et al. presented a photogrammetric technique for structural surveying and modeling of a castle case study in Italy. From the geometrical survey, the model of

the castle in a 3D polygon mesh format was constructed and adjusted using PhotoScan software. Since the discrepancy of the generated surface mesh was expected, the mesh could not be directly moved to a FE analysis software. In order to eliminate the imperfections in the mesh, the 3D model was imported from PhotoScan to Geomagic Studio software in Standard Triangulation Language (STL) format, and “Mesh Doctor” feature was used in mesh repairing. The final step was to transfer the repaired 3D surface mesh from Geomagic to SAP2000 with the help of .dxf format in AutoCAD (Barrille et al., 2015). In the previous mentioned work, only surface mesh with simplified thickness assumptions was generated by the integration of many tools with different formats.

Hinks, et al., (2012) explained two main problems related to surface finite element modeling of complex structures: inaccuracy and high user efforts. Thus, a 3D-solid FEM generation tool was required for faster and more accurate geometrical representation of structures. Hinks, et al. presented an automated method to generate 3D solid models of structural walls by using voxel grids.

For the evaluation purpose of the stone columns of a historic cistern in Turkey, the integration of FARO Scene, Geomagic and Hypermesh software led to the generation of a detailed tetrahedral finite element model using the geometrical scanning survey of the columns (Almac et al., 2015). Generally, to convert a surface mesh model created from TLS data to a 3D solid FE model, a special software (for example Geomagic, Gmsh, Tetgen, and Autodesk Recap) can be used in a time and effort-consuming process and using watertight model with suitable formats (Korumaz, et al., 2017).

As mentioned in Castellazzi et al., 2015, there is a lack of point clouds to solid FEM transformation procedures for complex historical structures. Thereby, a semi-automatic numerical modeling of 3D finite element mesh based on surveyed point clouds of historical complex buildings (CLOUD2FEM) was developed by Castellazzi et al., 2015. The aim of the research was to minimize the time and labor effort needed

to build FE models of complex monumental structures compared to a traditional time-consuming CAD-based process in converting TLS surveys to accurate FE models. CLOUD2FEM procedure was based on several steps to convert a geometrical survey to volumetric mesh. Firstly, the point cloud of a historical building was sampled using “Poisson Disk Sampling”, cleaned, post-processed and divided, using GIS software, into regular slices of small increments to preserve the accuracy of building shape. These slices were used to prepare the point cloud and keep the set of points which represent the internal and external boundaries of building. Then, “concave hull algorithm” was used to categorize and connect the points of each slice forming internal and external polygons. By subtracting the two boundary polygons, the areas correspond to each section of geometry were obtained and converted to a digital image with adequate resolution. Next, every pixel of the digital image was represented by a volume element (voxel) that was easily transformed to eight-node hexahedral element. Finally, the full 3D FEM of part of the complex large-scale building was achieved by stacking all the layers of finite elements. Due to operator-intensive and time-consuming slicing and splitting process which related to total number of slices to be processed, Bitelli et al., (2016) developed the approach by the examination of geometrical variation between adjacent slices, and thus a reduction in the number of slices to be processed is achieved.

The previous semi-automatic strategy can be considered as a breakthrough in point cloud to FE modeling of historical culture. However, as mentioned above, slicing process, boundaries creation and digital imaging is a time-consuming and labor-intensive approach. Therefore, a new automatic methodology to directly generate FE model with solid mesh from TLS surveys of cultural heritage is developed and validated in this thesis.

1.3. Objective and Scope

The main purpose for this study is to develop an algorithm and software for 3D solid finite element model generation using laser scanning data of complex historical structures. The secondary aim is to generate 3D FEM of Şehzade Mosque located in Istanbul and carry out earthquake vulnerability assessment using linear analysis.

For historical structures of complicated geometry or structures with lack of plans and documents, terrestrial laser scanners (TLS) are used to expeditiously capture the complete shape and details by recording millions of point coordinates known as “point clouds”. In this study the point cloud is used for the 3D generation of solid finite element models (FEM) by automatically generate borders and determine internal volumes to be filled using cubic solid members, hexahedrons.

The laser scan data for complex structures such as a masonry arch bridge and a historic mosque are obtained and used to test the developed algorithm and MATLAB code. A 3D shell FEM of pilot structure (Şehzade Mosque) is constructed and calibrated using field test dynamic data, then the structural behavior of Şehzade Mosque under dead and earthquake loads is investigated and compared for both 3D shell and solid FE models.

1.4. Laser Scanning and Data Pre-Processing

Laser scanning surveys of historical structures are usually applied for the documentation, drawings preparation, vulnerability assessment and rehabilitation of cultural heritage.

Laser scanners are geometrical acquisition tools to expeditiously capture the entire shape of a building with several scan positions. Time of flight laser (TOF) scanners use the time needed for a laser beam to reach a surface point and reflect back in position calculation. Thousands of point coordinates (x, y, z) for the surveyed object can be recorded per second with a precession of few millimeters. The output of laser

scanning survey is generally called a point cloud, millions of 3D coordinates represent the shape of a scanned object.

In this study the inside and outside survey data of historical structures are used to automatically generate a 3D- solid finite element model.

Before using scan data to generate 3D-solid FE models, the following phases are carried out to process point clouds:

1. Data Registration: The alignment of laser scans, captured from different viewpoints, or “point cloud registration” can be done with available specialized software such as FARO Scene, PhotoScan, CloudWorx, CloudCompare and Cyclone. Figure 1.3 shows an example of two laser scans alignment.

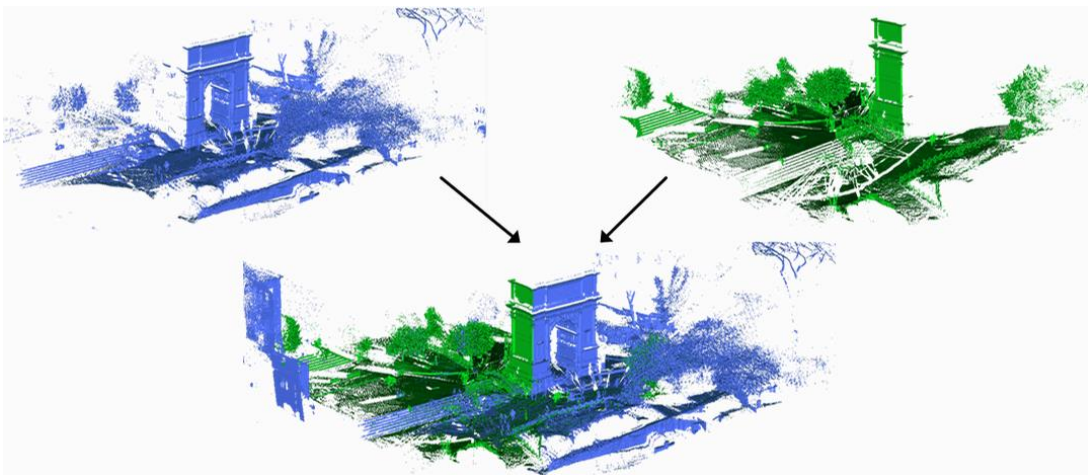


Figure 1.3. Example of two scans registration (Theiler and Schindler, 2012)

2. Ground & trees detection: “Cloth Simulation Filter” in CloudCompare software is used in this study for the detection and removal of terrain, ground and trees from cloud data. The simplest format of cloud data .txt file can be imported to the software at this stage.
3. Cleaning: At this stage, only the structural point cloud is remained. Some undesired features such as furniture, cables and other non-structural elements

should be removed using MeshLab, CloudCompare, 3DReshaper...etc. Furthermore, for point clouds of monumental complex structures, a segmentation tool in CloudCompare can be used to slice the point cloud into enough number of cross sections (e.g. 5 slices) which makes the cleaning process easier and more efficient.

4. Triangulation: Triangulation or surface meshing is a necessary step before repairing surface and filling holes caused by the missing data of unreachable parts of a structure. Examples of software for surface construction (triangulation) are MeshLab, Gmesh and 3DReshaper.
5. Holes filling: After surface construction using scan data, the holes in structure can be filled using MeshLab, PhotoScan, or 3DReshaper. It is important to mention that for the proposed 3D-solid FEM generator using only the 3D generation approach discussed in section 2.2.2, the bottom edges of internal and external surfaces of the structure should be matched together forming one 3D surface shape of the structure instead of two surfaces.
6. Data sampling: Sampling points from the 3D surface prepared in phase 5 is done to ensure regular distribution of points, and to record new points for the filled surface of holes. CloudCompare software has “sample points on a mesh” feature for sampling points from a surface mesh.

A new, cleaned and repaired point cloud of a scanned structure is obtained at the end of the pre-processing methodology. The integration of 3DReshaper-CloudCompare is sufficient and recommended by this research to fulfill the point cloud preparation for FE model generation.

CHAPTER 2

AUTOMATED 3D SOLID FEM GENERATOR

Once the repaired point cloud for the entire structure is available, including inside and outside survey data, a three-dimensional finite element model with volumetric mesh can be generated. In this chapter, an algorithm that generates 3D-Solid FEM for the structure using the scan data is devised. First, the boundaries of the structure are defined using the scan data. Then, the thickness of structural elements is defined with internal solid mesh using the algorithm described in section 2.3. Finally, the overall boundary and internal solid finite elements are generated to be used in FE model analysis. The algorithm is summarized in the flowchart of Figure 2.3.

To simplify the algorithm demonstration, simple-hypothetical scan data of totally 200000 points for a dome with 14-m diameter is utilized as shown in Figure 2.1.

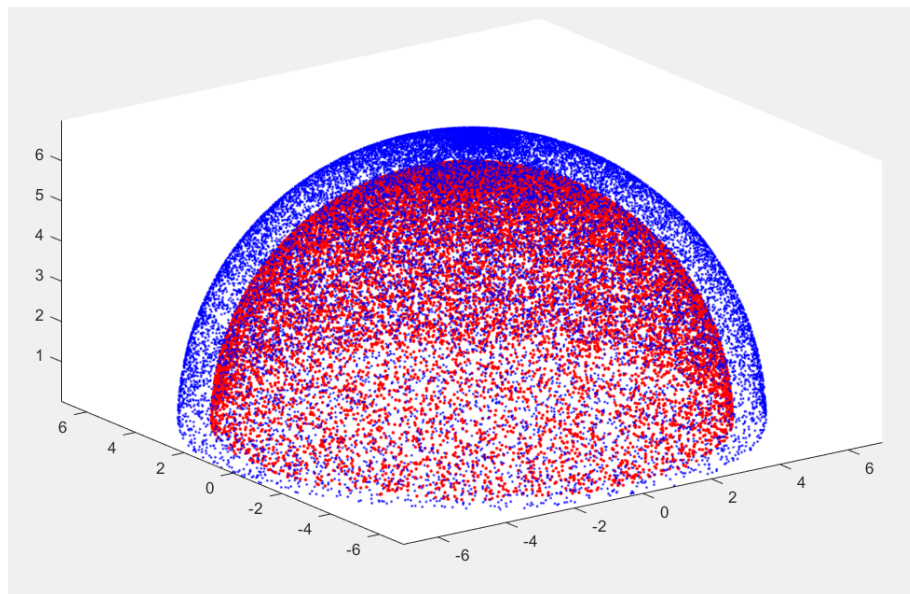


Figure 2.1. Hypothetical scan data

2.1. Defining Boundary Solids Using Scan Data (Mapping)

The flowchart in Figure 2.3 is divided into three main phases which describe the phases of the generator algorithm. In this section, the first phase is explained as follows:

2.1.1. Scan Data Reading and Parameters Definition

- Given a repaired cloud, the coordinates $x, y,$ and z of points are inserted into an $N \times 3$ matrix, where N is the total number of points. The label of each point, n is the corresponding row number in the array.
- Minimum and maximum $x, y,$ and z coordinates among all data are defined and labeled as $x_{min}, y_{min}, z_{min}, x_{max}, y_{max},$ and z_{max} .
- Generally, the coordinates of data points in a laser scanning survey are measured relative to the global “Geographic Coordinate System”. For more convenient usage of coordinates, they can be transferred with respect to the origin point $(0, 0, 0)$ by subtracting $x_{min}, y_{min},$ and z_{min} from $x, y,$ and z coordinates for each data point.
- The size of a solid finite element with 8 nodes and six faces (also called cubic hexahedron) can be chosen according to the intended resolution of the generated FEM. The size of the cube can be defined by Δ parameter (cube volume is Δ^3).
- As shown in Figure 2.2, a 3D network of virtual mesh is assumed with Δ dimension for the finite element. Number of virtual cubes in $X, Y,$ and Z directions are calculated using the following equations:

$$n_x = \frac{\text{round}(x_{max} - x_{min})}{\Delta} + 2 \quad (2.1)$$

$$n_y = \frac{\text{round}(y_{max} - y_{min})}{\Delta} + 2 \quad (2.2)$$

$$n_z = \frac{\text{round}(z_{max} - z_{min})}{\Delta} + 2 \quad (2.3)$$

Where n_x, n_y and n_z are the number virtual cubes in X, Y , and Z directions, $x_{max} - x_{min}$, $y_{max} - y_{min}$, and $z_{max} - z_{min}$ are the ranges of x, y , and z coordinate values of data points. Two extra cubes are added in the previous equations in each X, Y , and Z directions to enclose the entire object in a larger bounding volume. The total number of virtual boxes is $n_x \times n_y \times n_z$.

- i, j , and k indices are used to refer to a certain box in the virtual mesh network relative to X, Y , and Z .

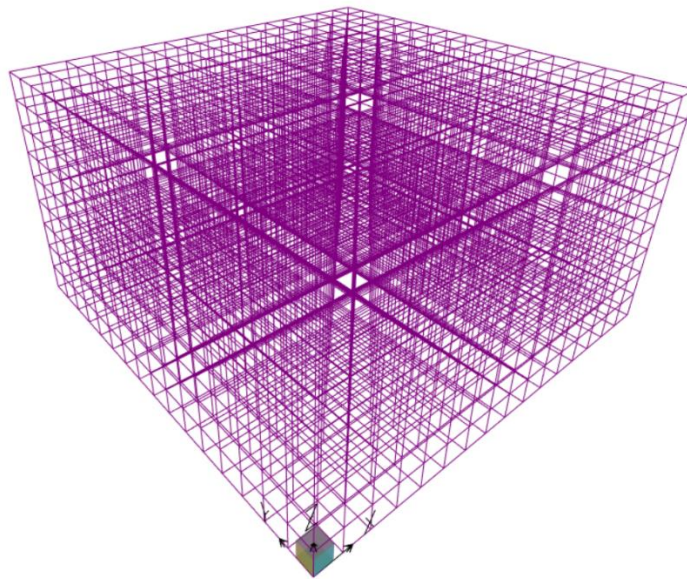


Figure 2.2. A 3D mesh of virtual cubes ($\Delta=1$ m)

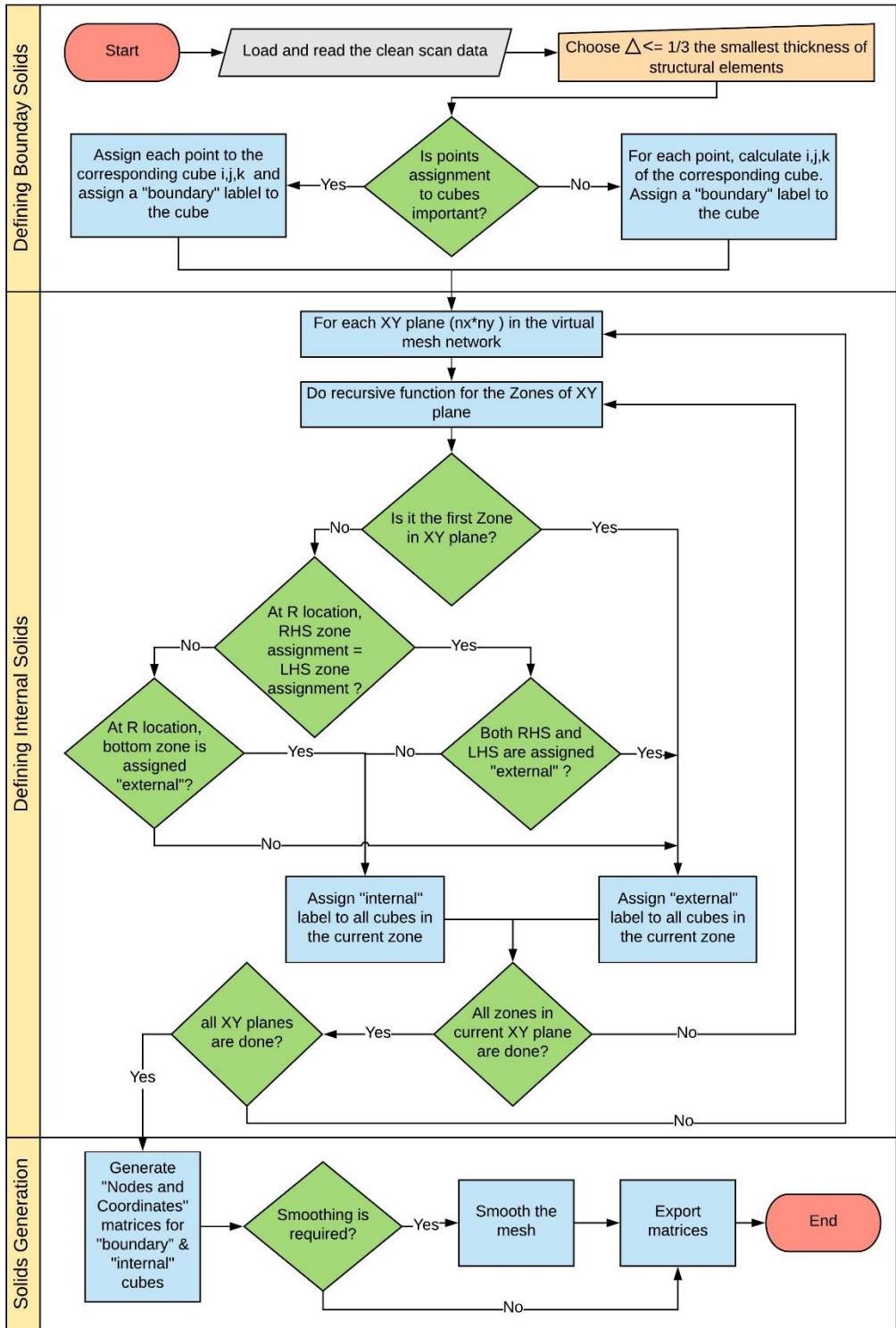


Figure 2.3. The flowchart for the generator algorithm using 2D navigation for internal solids definition

In phase 1 of the algorithm, each point in the cloud is related to a certain boundary cube with at least one data point inside. This process is called mapping and performed in two approaches as follows:

2.1.2. Boundary Mapping with Points

This approach is applied when it is important to know all the points inside a certain box. For each point $p_i = (x_i, y_i, z_i)$, the i, j , and k indices of the corresponding cube are calculated using equations 2.4, 2.5 and 2.6. The i, j, k values for cubes can range from 1, 1, 1 to n_x, n_y, n_z . Afterward, the point p_i is assigned to the corresponding i, j, k cube and the cube is assigned as a “boundary” cube. This process is repeated until each cloud data point is assigned to the appropriate cube.

$$i = \lfloor \frac{x_i - x_{min}}{\Delta} + 2 \rfloor \quad (2.4)$$

$$j = \lfloor \frac{y_i - y_{min}}{\Delta} + 2 \rfloor \quad (2.5)$$

$$k = \lfloor \frac{z_i - z_{min}}{\Delta} + 2 \rfloor \quad (2.6)$$

If a point has the minimum coordinates, $p_i = (x_{min}, y_{min}, z_{min})$, then the cube indices are (2, 2, 2) and any cube with indices less than 2 is an extra virtual cube as mentioned in section 2.1.1.

2.1.3. Boundary Mapping Without Points

When it is not necessary to know which points are related to a specific cube, the previous approach is valid but the assignment of points to cubes is skipped.

Only the cube with points inside is assigned as a “boundary” cube. For each point $p_i = (x_i, y_i, z_i)$, the i, j , and k indices of the corresponding cube are calculated and a “boundary” label is assigned to the cube. While other cubes which have no points are not given a “boundary” label. At the end of phase 1, all the inside and outside boundary cubes of the scanned object are defined. Figure 2.4 shows an example of the boundary cubes of the dome after generation.

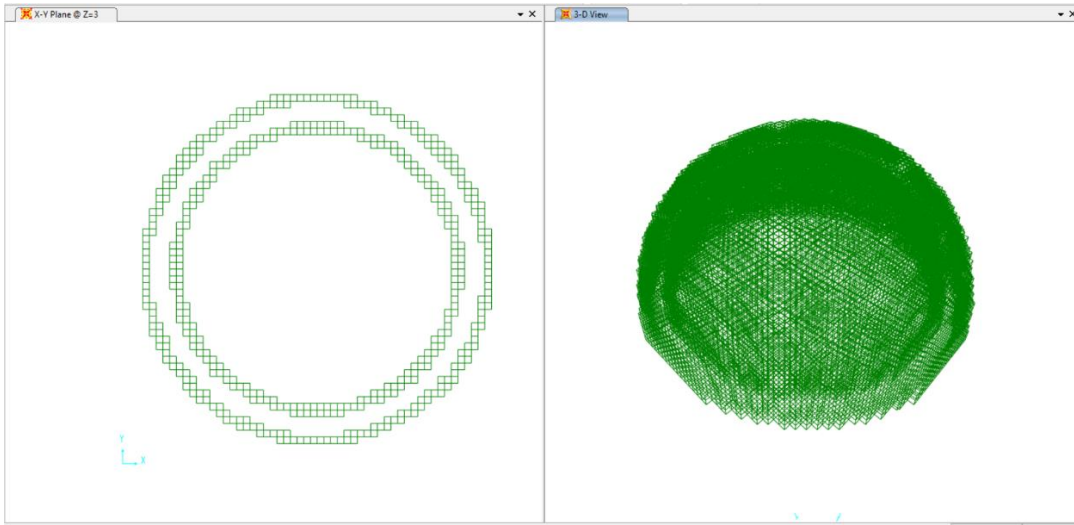


Figure 2.2. The boundary cubes of the dome ($\Delta=0.25$ m)

2.2. Defining Internal Solids

Phase 2 of the 3D-solid FEM generator is applied to define the internal cubes which represent the thickness of structural elements. Each non “*boundary*” cube in the virtual mesh might be “*internal*” cube: between the mapped boundaries, or “*external*” cube: outside the two boundaries. Only boundaries and “*internal*” cubes have to be generated as finite elements to represent the entire 3D model of the structure. As summarized in phase 2 in the flowcharts of figures 2.3 and 2.7, two approaches for defining “*internal*” cubes are proposed based on 2D or 3D navigation through the virtual mesh with the help of boundaries defined in phase 1. The “*internal*” and “*boundary*” cubes are only generated at the final stage of solid modeling.

2.2.1. 2D-Navigation Approach for Internal Mesh Definition

Generally, and not similar to a simple dome, historical structures can have several rooms. The outer space of the structure, the thickness of each structural element, and the spaces inside rooms are named as zones as shown in Figure 2.5. The 2D navigation approach for internal mesh definition is summarized in the flowchart of Figure 2.3. In

order to decide whether the non “*boundary*” cube is “*internal*” or “*external*” cube, the following approach is applied for each 2D XY section:

- The 3D virtual mesh network in Figure 2.3 is regularly divided into XY planes with total number of planes equal to the number of cubes in Z direction, n_z . Thus, a moving virtual cube is used to navigate through each XY section of cubes and for each zone inside current XY section using “Recursive” function.
- A recursive function is a function that repeat itself several times. It is used in the 3D-solid FEM generator to call all cubes inside a zone. The recursive function orderly calls Zone 1, Zone 2 and Zone 3 cubes starting from the virtual cube R1, R2 and R3 respectively as shown in Figure 2.5. For each virtual cube in Zone 1, the surrounding cubes are added and called again by the function to add their surrounding cubes only within the current zone of XY section. The “*boundary*” cubes work as borders separating zones.
- The “*boundary*” cubes are utilized inside the recursive function as dividing borders between the zones. For each virtual cube, the function adds the surrounding non “*boundary*” cubes (i.e., adding 8 or less cubes around the current cube).

All cubes in Zone 1 are obviously considered as “*external*” cubes. However, for Zone 2, the left-hand side and right-hand side assignments of zones are compared to decide the assignment of Zone 2. In Zone 2 case, RHS and LHS cubes are in Zone 1 which are previously considered as “*external*”. Thus, Zone 2 assignment is the opposite, “*internal*”. This process is repeated for all zones of the XY section. Sometimes the bottom zone assignment is used as a second check when RHS and LHS assignment are different.

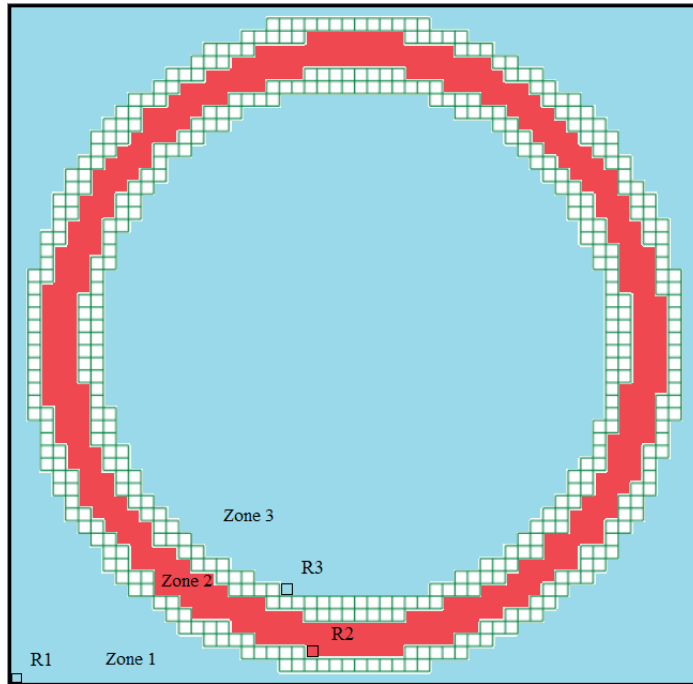


Figure 2.3. The distribution of zones, and starting cubes for the recursive function in an XY section of the dome

The major limitation for this method of mesh generation is Δ value. When the size of cube is larger than $\frac{1}{3}$ of the minimum thickness of elements, the inside and outside boundary cubes will not be separated, the number of zones between boundary cubes will increase and the zones won't be regularly distributed which will affect the accuracy of the proposed approach for the decision of “*internal*” or “*external*” assignment .

Therefore, the 3D navigation approach, which is presented in the next section and shown in the flowchart of Figure 2.7, guarantee the generation of cubic mesh regardless the size of finite element Δ .

2.2.2. 3D-Navigation Approach for Internal Mesh Definition

The 3D navigation approach for “*internal*” mesh definition can be applied with any value of Δ . Using this method, the outer space of a scanned structure and the spaces inside rooms are all named as Zone 1 while all the structural elements are considered

as Zone 2 as shown in the example of Figure 2.6. In order to decide whether the non “boundary” cubes are “internal” or “external”, the 3D navigation approach is applied for Zone 1 and Zone 2 as shown in the flowchart of Figure 2.7:

- A moving virtual cube is used to navigate through Zone 1 and Zone 2 using a recursive function that call all cubes inside the zone.
- The recursive function first calls Zone 1 cubes starting from the virtual cube 1,1,1 to all cubes in 3D surrounding the structural elements in the outer and inner spaces of the structure. The “boundary” cubes work as borders separating Zone 1 and Zone 2. All the cubes of Zone 1 are obviously considered as “external” cubes.
- After the end of the first recursive function, simply all the remaining virtual cubes, all cubes in Zone 2, are assigned as “internal” cubes. Figure 3.8 shows an example of the internal cubes for dome after generation.

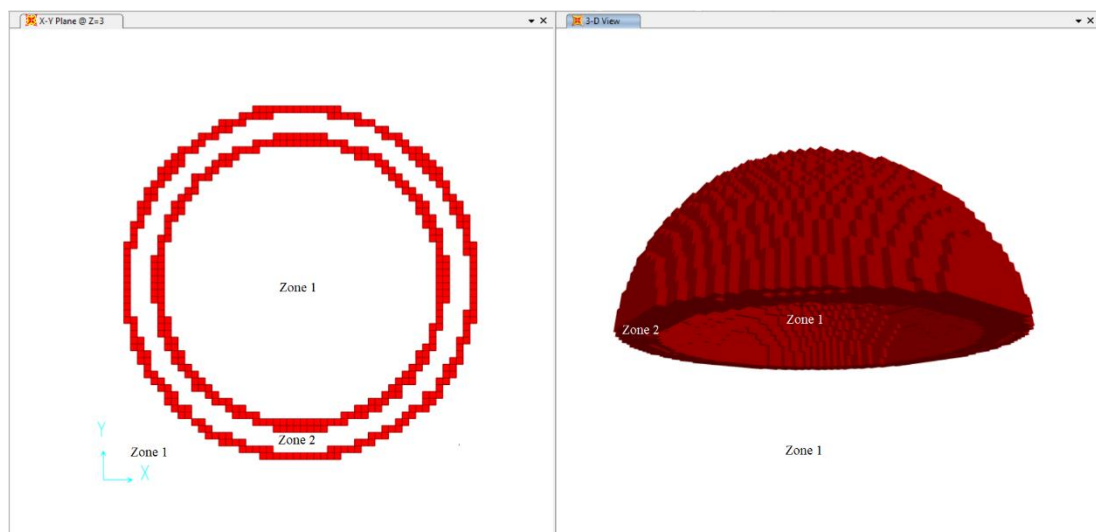


Figure 2.4. The distribution of zones when 3D navigation is used for the dome

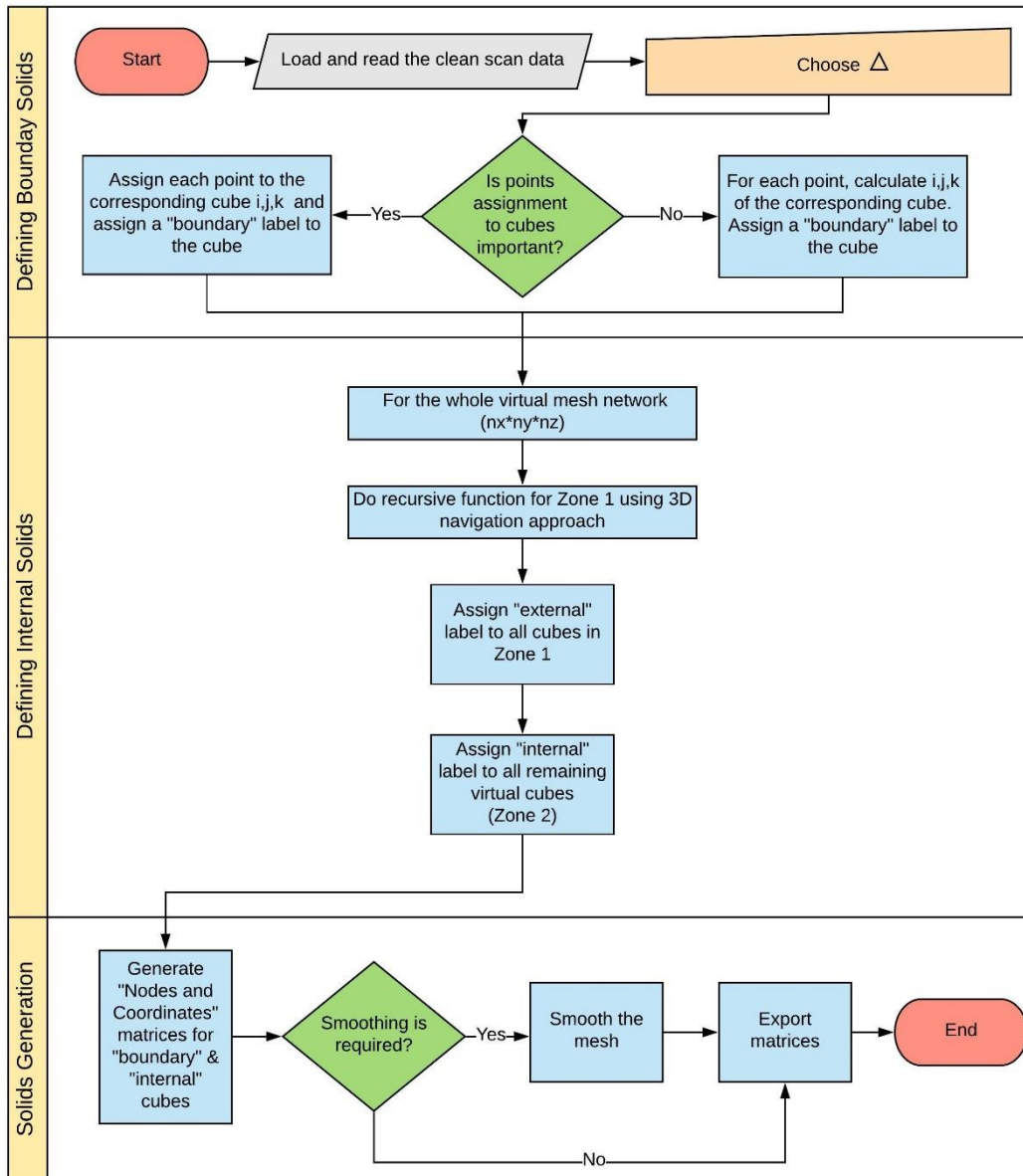


Figure 2.5. The flowchart for the generator algorithm using 3D navigation for internal solids definition

2.3. Finite Elements Generation

The type of finite element used in 3D mesh generation of this study is a regular solid (hexahedral element) with 8 nodes and 6 faces. After the “*boundary*” and “*internal*” solids are well defined in phase 1 and phase 2 of the algorithm, the matrices defining

the nodes and coordinates of hexahedrons are generated based on Δ and i, j, k indices for each cube. For instance, the node number and x, y , and z coordinates for Node 1 of an i, j, k cube are calculated using equations 2.7, 2.8, 2.9 and 2.10 respectively.

$$Node_1 = i + (j - 1) \times n_x + (k - 1) \times n_x \times n_y \quad (2.7)$$

$$coor_x = x_{min} + (i - 1) \times \Delta \quad (2.8)$$

$$coor_y = y_{min} + (j - 1) \times \Delta \quad (2.9)$$

$$coor_z = z_{min} + (k - 1) \times \Delta \quad (2.10)$$

The final matrices are then easily exported to a text file that might be imported to any available FE analysis tools. Figure 2.9 shows the full generated FE model for the dome with a FE size of 0.25m. The generated mesh can be improved using the smoothing algorithm described in section 2.5.

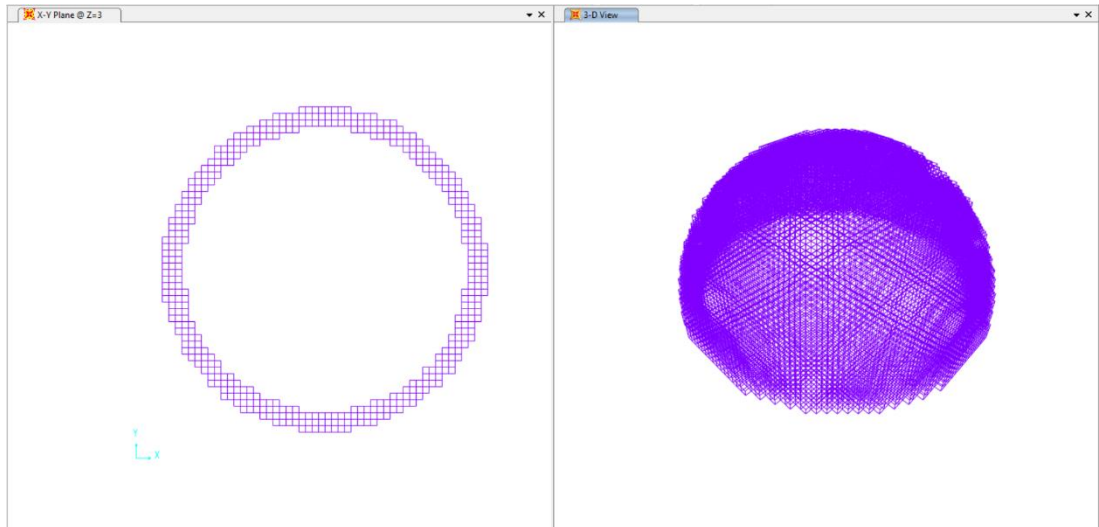


Figure 2.6. The internal boxes of the dome ($\Delta=0.25$ m)

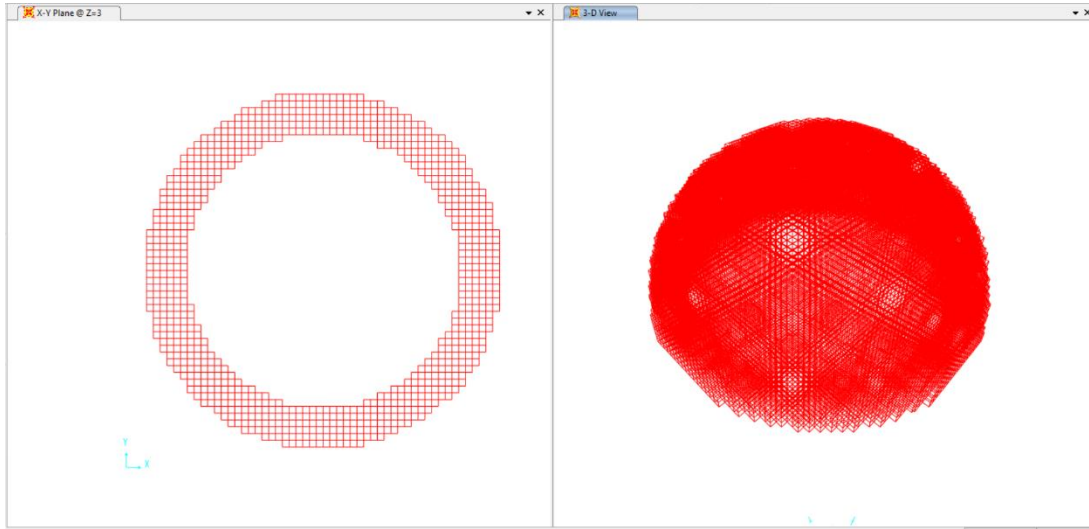


Figure 2.7. The boundaries and internal meshes of the dome ($\Delta=0.25$ m)

2.4. Time and Memory Efficiency Improvement

The algorithm efficiency is improved in several ways:

- Since a boundary cube can have a large number of points which depends on cloud density and cube size, the use of array data structure to organize points into corresponding cubes using i, j, k indices is not an efficient process in terms of time and memory. Therefore, a hash table, which can map several data points to a certain string key ' i, j, k ', is used instead of enormous array e.g. 4D array.
- When the recursive function is used for internal solids definition, for each recursive call, a copy of the function is allocated and pushed on the top of program stack. This operation is not efficient in terms of memory and usually leads to a memory overflow. The combination of recursive and iterative functions is applied by utilizing a FIFO (First In First Out) queue which deals separately and orderly with function calls without accumulating all the calls in the program stack at the same time.

- Pre-definition of an array size can significantly save run time. The number of variables for the array is first calculated to define the array size before the insertion of data.
- Since millions of points are processed in the 3D solid generator, out-of-memory error is expected during model generation. This can be solved by sequentially clear unnecessary data for each phase of generation.

2.5. Finite Element Model Smoothing

When a small value of Δ parameter is set to define the mesh size in the proposed 3D FEM generator, the acquired accuracy is adequate for performance analysis of monumental structures. However, a very fine mesh can diverge and prone errors to analysis results, a convergence sensitivity analysis is performed in 3.2.3.3. However, to solve the faceting in 3D model resulted from cubic mesh, it is possible to improve the mesh and adjust solid faces using a smoothing algorithm such as “TAUBIN Smoothing” (Castellazzi et al., 2015). TAUBIN smoothing is based on low-pass filter for the smoothing of piece-wise linear shapes such as tetrahedron and hexahedron faces (Taubin, 2015).

CHAPTER 3

GENERATOR VALIDATION: CASE STUDIES

In order to test and validate the developed 3D solid FEM generator, the generation of FE model of two case studies using the proposed approach is presented in this chapter. For the case study of Şehzade Mosque, the 3D solid FE model is compared to a 3D shell model and both models are calibrated using in-situ dynamic behavior test.

3.1. A Masonry Bridge FEM Generation

The laser scan data of a historical masonry bridge in Onaç village - Turkey shown in Figure 3.1, is used to validate the 3D solid FE generator of this study. The total number of data points before pre-processing is about 2.5 million. The length and width of the bridge are 30m and 2.8 m respectively.



Figure 3.1. Onaç Masonry Bridge (YAVUZ MİMARLIK, 2017)

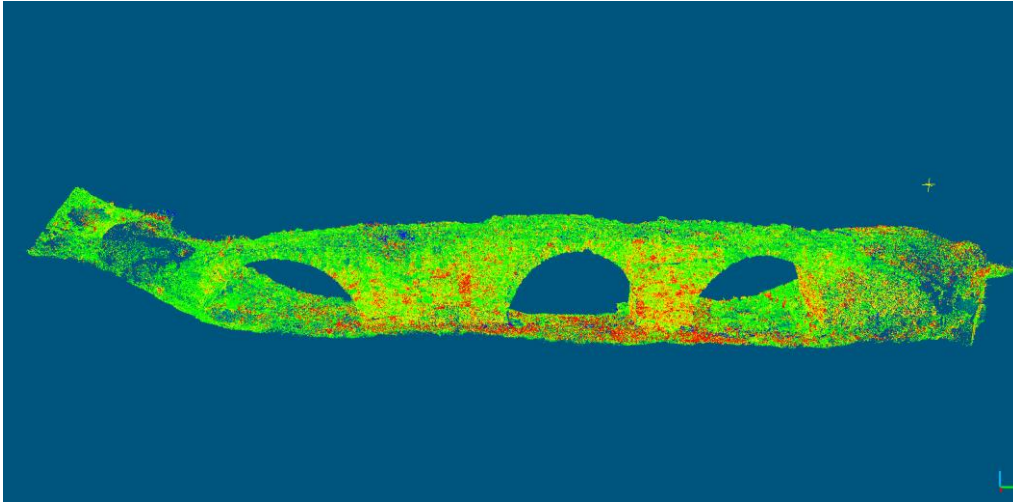


Figure 3.2. The scan data of Onaç masonry bridge

The solid FE model for the bridge is generated using the following steps:

1. The cloud representing the ground is detected and removed using CloudCompare tool, the entire cloud is cleaned, saved as text file and imported to 3DReshaper software as shown in Figure 3.3.
2. In 3DReshaper software, the cloud is sampled to 200,000 points, a surface mesh is constructed and the holes in surface mesh are detected and filled. Afterwards, the mesh shown in Figure 3.4 is exported in Standard Triangulation Language (STL) format.

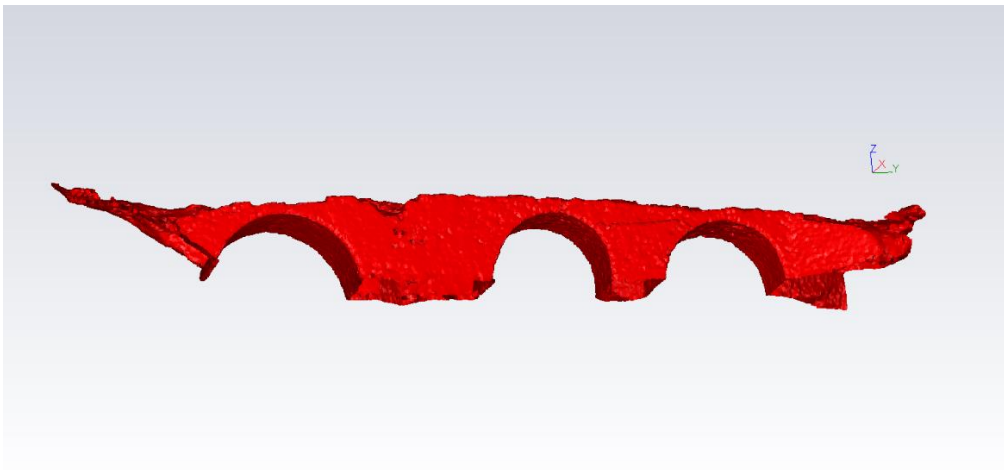


Figure 3.3. The clean cloud of Onaç masonry bridge

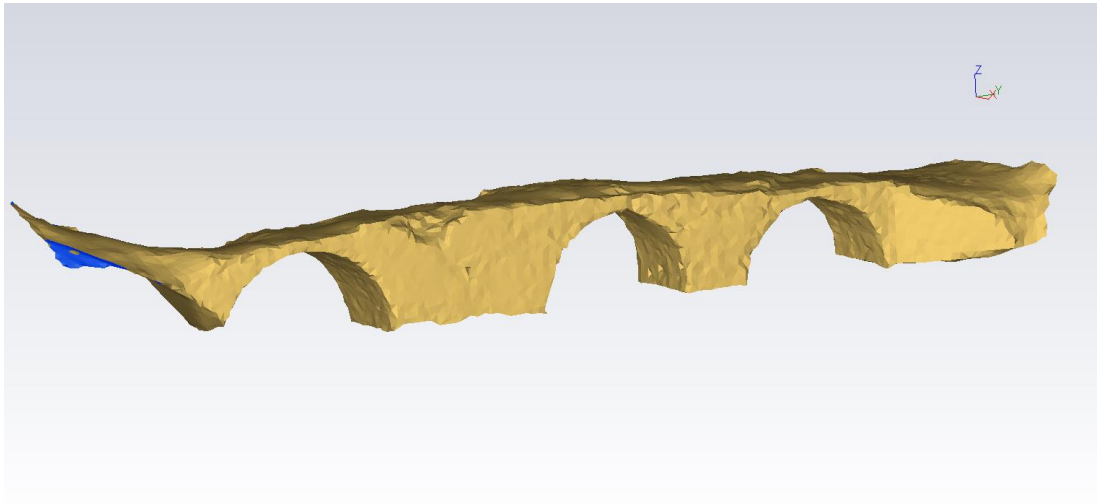


Figure 3.4. The surface mesh for Onaç masonry bridge

3. In order to have data points that represent the filled holes, the surface mesh is again imported to CloudCompare in STL format and new point cloud of 800,000 points is sampled from the surface mesh as shown in Figure 3.5.



Figure 3.5. The final cloud of Onaç masonry bridge

4. Afterwards, the 3D solid generator of this study is implemented using MATLAB and used to generate the volumetric finite element model of Onaç masonry bridge with 0.2 m increments of solid hexahedral mesh (cubes).

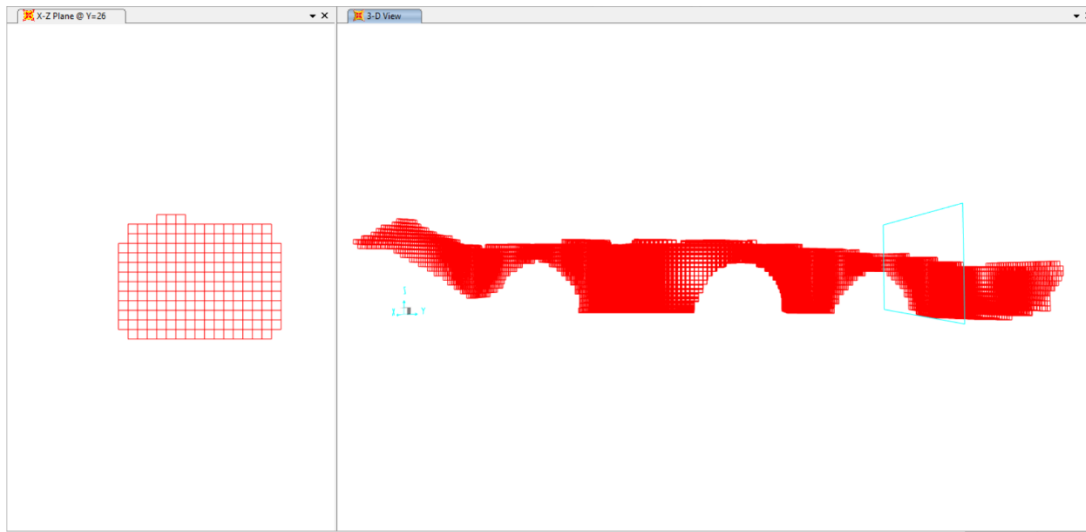


Figure 3.6. The 3D hexahedral FE model of Onaç masonry bridge ($\Delta=0.2$ m)

3.2. Şehzade Mosque Modeling and Analysis

Due to vibration load caused by opening a new metro line near Şehzade Mosque, deterioration of materials and the need for performance validation under future earthquakes, the structural behavior and dynamic response study is planned for Şehzade Mosque and the finite element modeling and analysis together with in-situ dynamic testing are performed. In this study, 3D - shell finite element model and 3D-volumetric FE model are presented with comparison of analysis results. The in-situ dynamic measurements are used to calibrate the numerical models.

Şehzade mosque or "Prince's Mosque" is located in Fatih district in Istanbul. The mosque was designed by Sinan architect and built by the commanding of "Suleiman the Magnificent" in 16th century. The main structure of the mosque has a square plan with the longest span of 50 m, a central large dome with a diameter of 19 m supported by four columns with 26 m height and bounded by four half-domes and a pair of minarets with 50 m height. The mosque also has a courtyard bordered by 16 domes. Due to the geometrical complexity of the mosque and lack of accurate drawings, laser scanning is utilized to facilitate the documentation and modeling of the structure. Figure 3.7 shows the general view of Şehzade mosque:

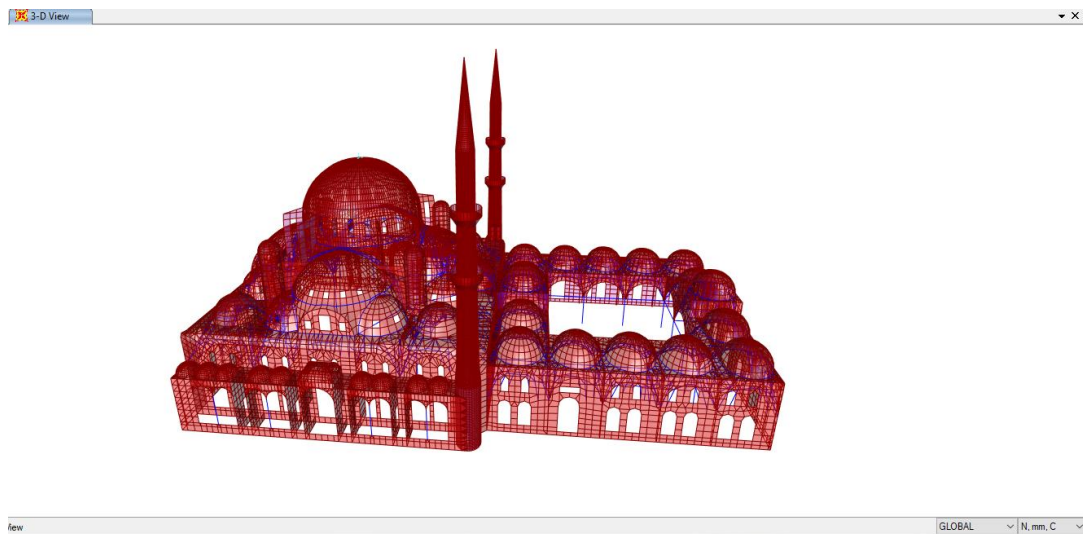


Figure 3.7. The general view of Şehzade Mosque- Istanbul

3D finite element modeling and analysis of Şehzade mosque are required for performance analysis and preservation of the historical masonry structure. Shell and solid FE models for the mosque are built as described in the following sections.

3.2.1. 3D-Shell Finite Element Model

Figure 3.8 shows the 3D - shell finite element model for the monumental masonry structure, Şehzade mosque, which is built and meshed in more than 2 weeks using SAP2000 program.



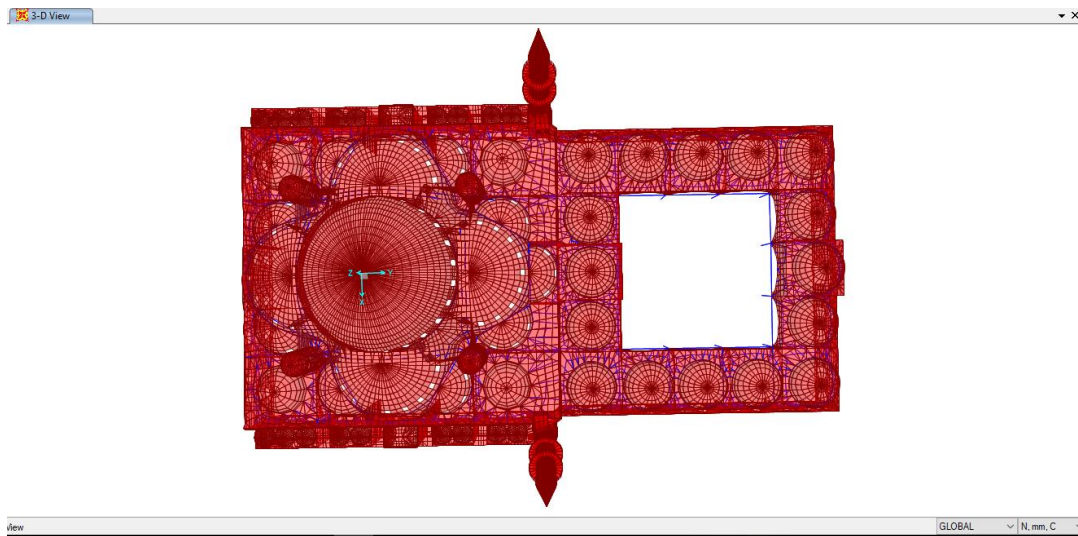


Figure 3.8. 3D shell model of Şehzade mosque

Due to the geometrical complexity as shown in Figure 3.9, some simplifications are made to model the structure using frame and shell members:

- In order to model the pendentives at corners and spandrels, a network of vertical steel members with 10 by 10 cm dimensions is used below secondary domes of the main structure and courtyard as shown in Figure 3.10.



Figure 3.9. Internal and external complex geometry of Şehzade mosque

- Rings of different size are used to model the frames surrounding the domes as shown in Figure 3.11.
- Since frame and shell members are used in modeling, some very rigid members are added to compensate the loss in thickness of structural elements at dome to wall and dome to main column connections as shown in Figure 3.12.

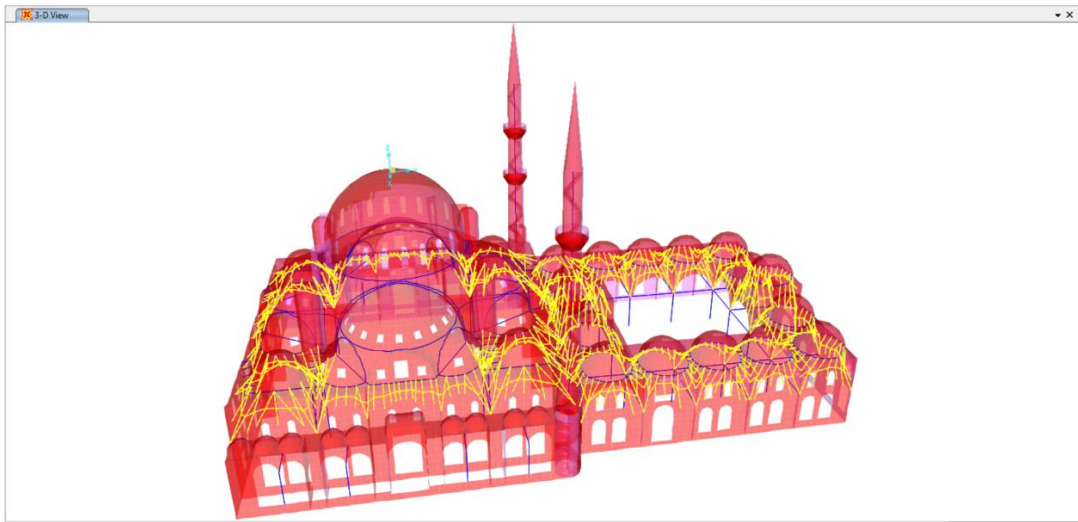


Figure 3.10. Frames used to model spandrels and pendentives

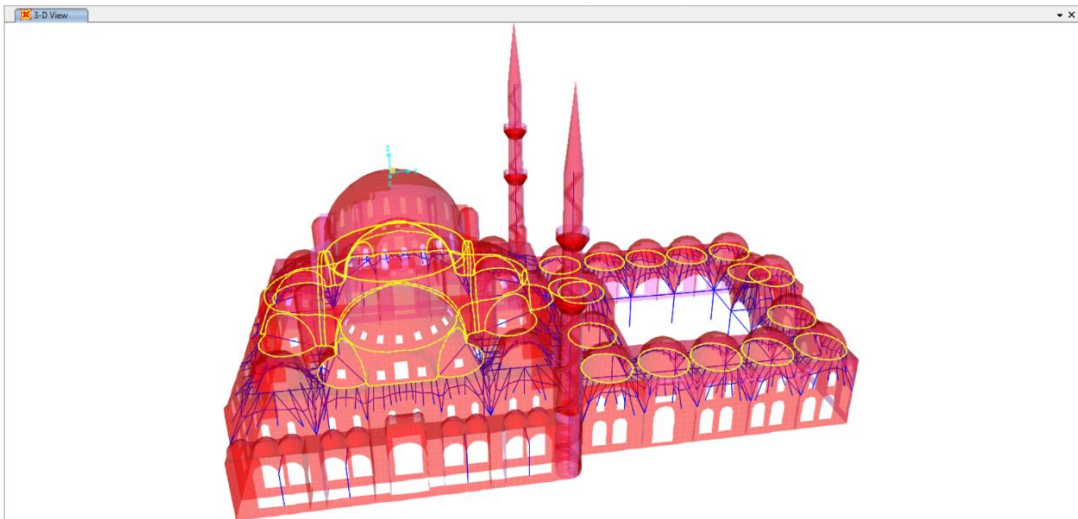


Figure 3.11. Rings used to model the surrounding frames for domes

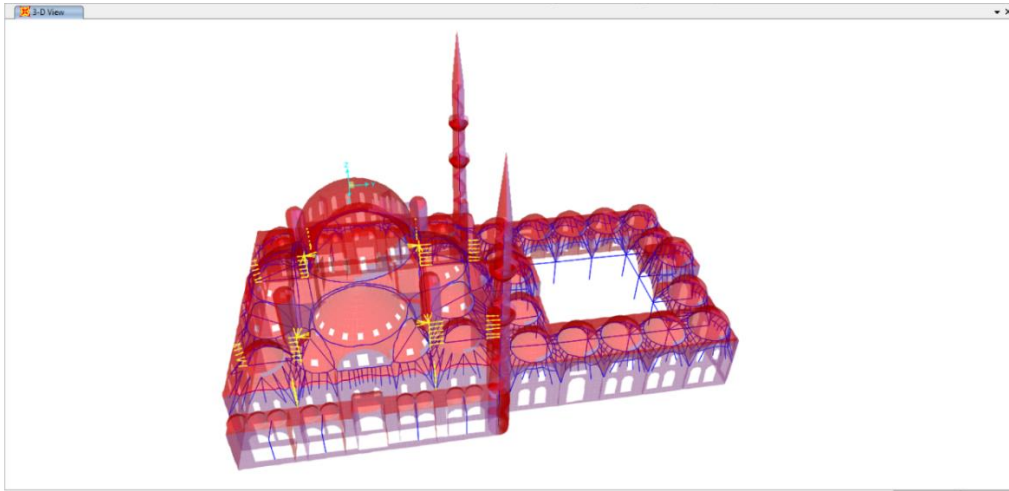


Figure 3.12. Rigid members for dome to wall and dome to column connections

Materials, loads, support definition and analysis results are presented in section 3.2.3.

3.2.2. 3D-Solid FE Model

The historical structure of Şehzade mosque in Istanbul -Turkey is planned to be assessed and prepared to resist earthquakes. The structure is mapped and several “point clouds” are recorded using terrestrial laser scanning survey TLS. The TLS of the mosque is accomplished by YÜKSEL Project Inc. with a precision of few millimeters and point to point distance of 10 cm, different scans inside and around the structure are captured, aligned and merged together. Figure 3.13 shows the scans of Şehzade Mosque after registration (alignment).

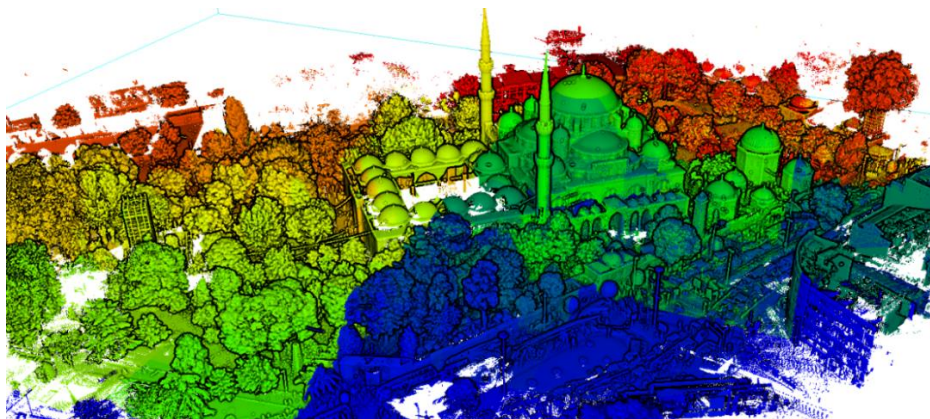


Figure 3.13. Registration of the scans of Şehzade mosque

The laser scan data of the historical masonry mosque in Istanbul - Turkey is used to validate the 3D solid FE generator of this study. The solid FE model is generated using the following steps:

1. The entire cloud is cleaned to only keep the data of the mosque. The data points for the mosque itself are more than 6 million for inside and outside point clouds. The cloud representing the ground is detected and removed using CloudCompare tool. Then, the inside and outside clouds are sliced into 5-7 slices to facilitate the cleaning of noise and cloud of non-structural parts. Since more than 50% of the minarets and side terraces scan data are missed and can't be repaired, the related clouds are removed. The inside and outside clouds before and after slicing and cleaning are shown in figures 3.14-16. The slices are saved as text files and imported to 3DReshaper software as shown in Figure 3.16.

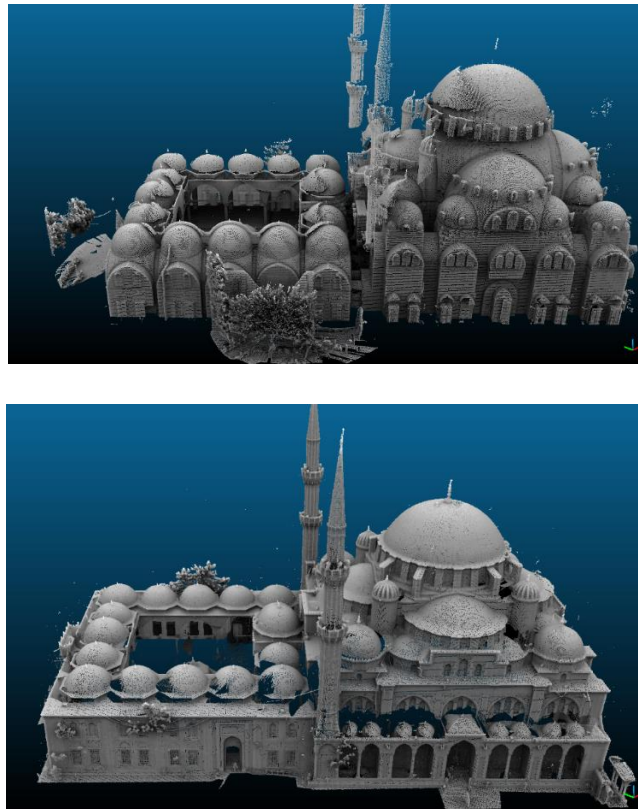


Figure 3.14. Inside and outside scans of Şehzade mosque

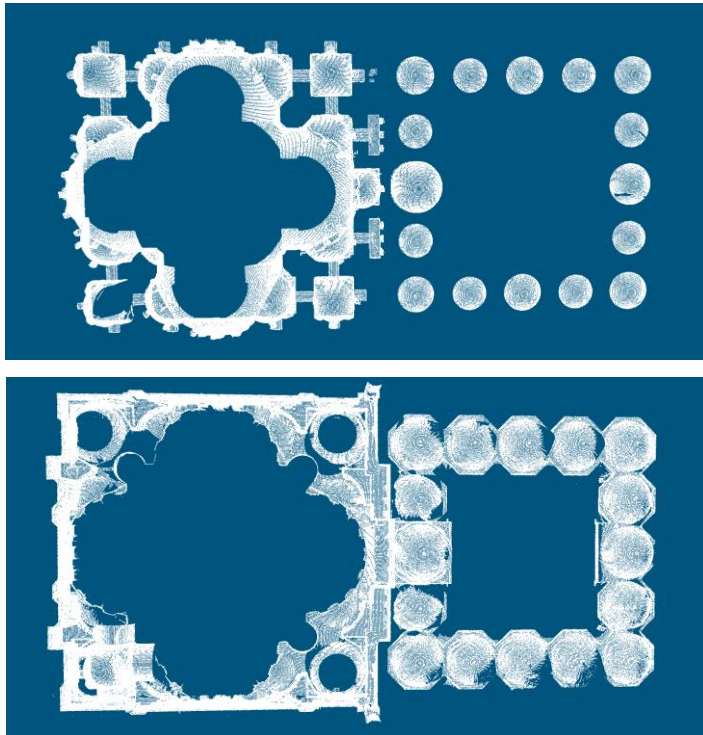


Figure 3.15. Slice 3 of inside and outside scans after cleaning

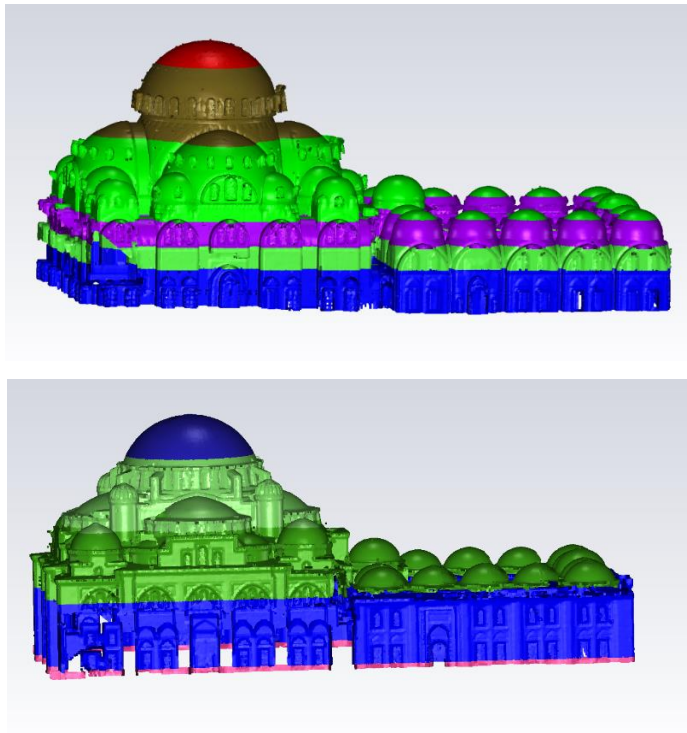


Figure 3.16. The slices of inside and outside scans after cleaning

2. In 3DReshaper software, the cloud is sampled from 6 to 2 million of points, a surface mesh is constructed and the holes in surface mesh are detected and filled using the powerful “bridge” and “fill holes” tools of 3DReshaper software. Afterwards, the mesh shown in Figure 3.17 is exported in Standard Triangulation Language (STL) format.
3. In order to have data points that represent the filled holes, the surface mesh is again imported to CloudCompare in STL format and new point cloud with a density of 200 pts/m² (4 million points) is sampled from the surface mesh as shown in Figure 3.18.

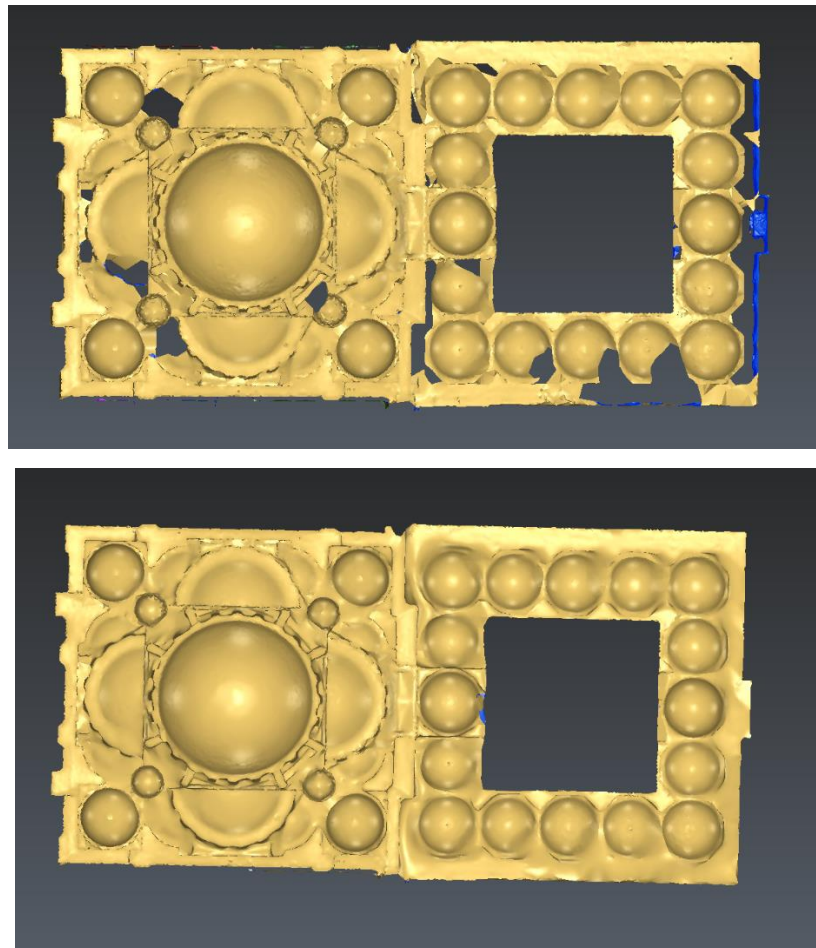


Figure 3.17. Outside surface mesh before and after healing

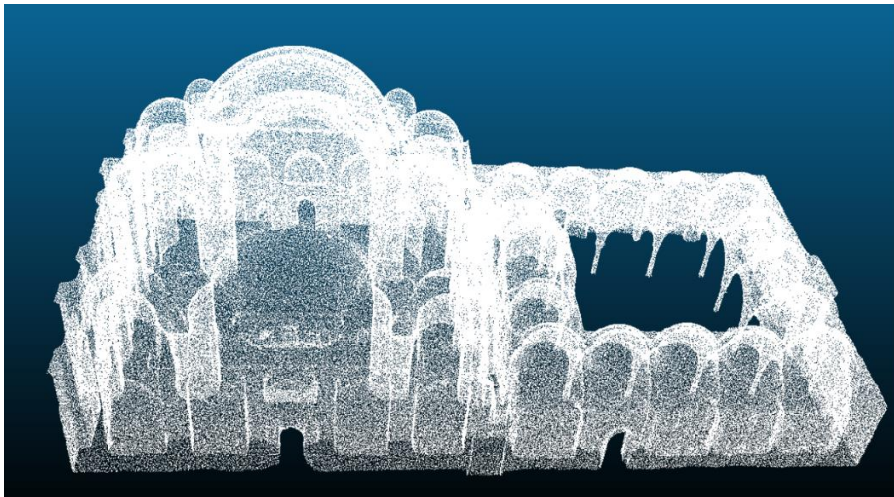
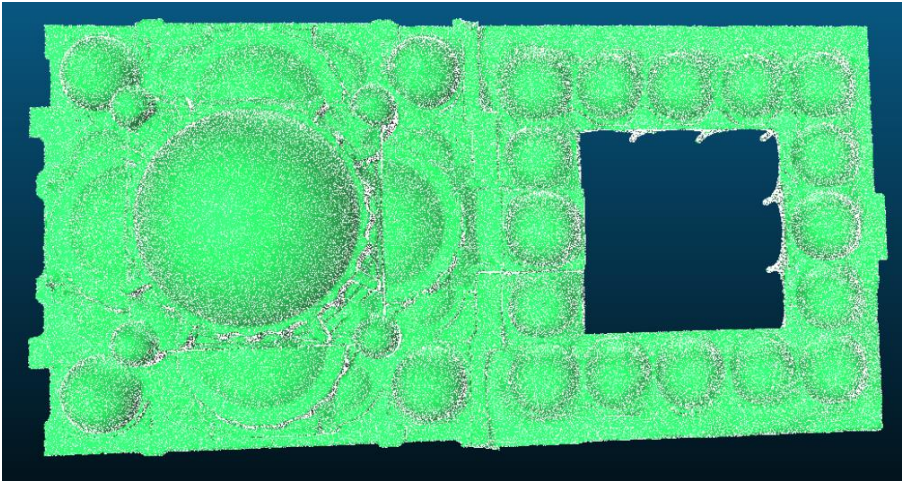
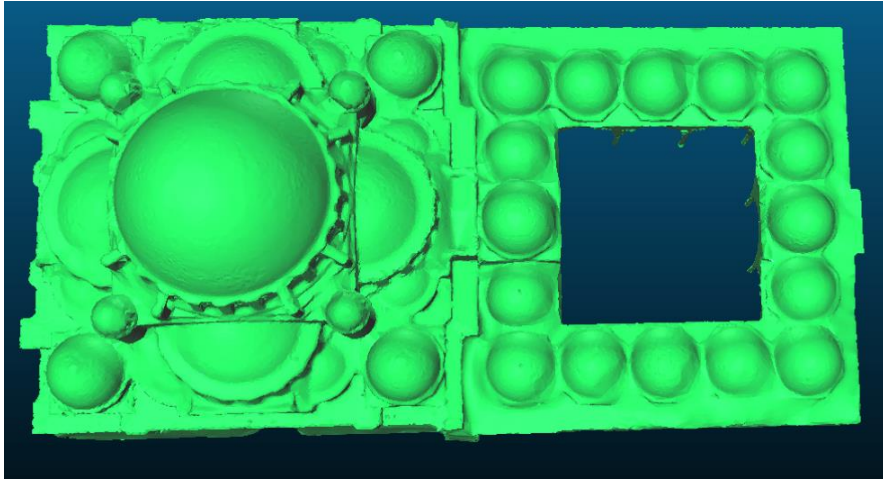


Figure 3.18. The final cloud sampled from the repaired surface mesh

4. Afterwards, the 3D solid generator is used to generate the volumetric finite element model of Şehzade mosque with 0.2 m solid dimension. The nodes and coordinates matrices are written to a “.s2k” text file of SAP2000 program.

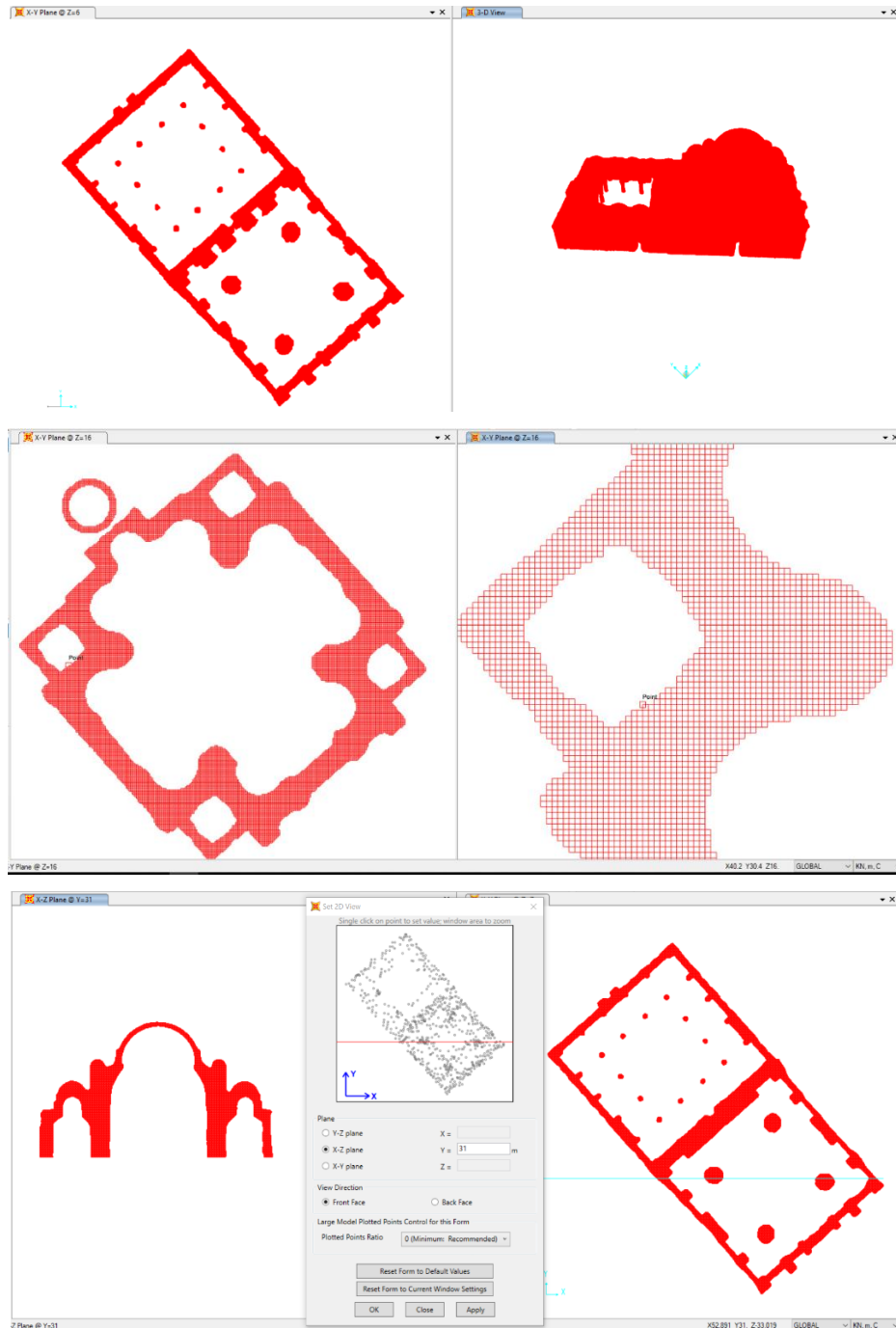


Figure 3.19. The 3D hexahedral FE model of Şehzade mosque ($\Delta=0.2$ m)

3.2.3. Dynamic Testing and Analysis Results

In order to calibrate the 3D shell and solid models of Şehzade mosque, accelerometers are used to measure the modal frequencies of the mosque. In this section, dynamic test results, calibration of shell and solid models, and analysis results are discussed and compared.

3.2.3.1. Dynamic Test Result

Using ambient vibration loads, several accelerometers were installed at the minarets and main dome to collect modal frequencies. The first mode frequencies obtained by in-situ dynamic tests of the minarets in both x and y directions are shown in Figure 3.20. Also, 4 in-situ dynamic tests were applied to the main dome, Figure 3.21 illustrates frequency versus amplitude record for one test done on the dome. The average for first modal frequency was found to be 1.15 Hz or a period of 0.85 s. Modal frequencies are used to calibrate shell and solid models by defining material properties, modulus of elasticity and unit weight, for structural elements.

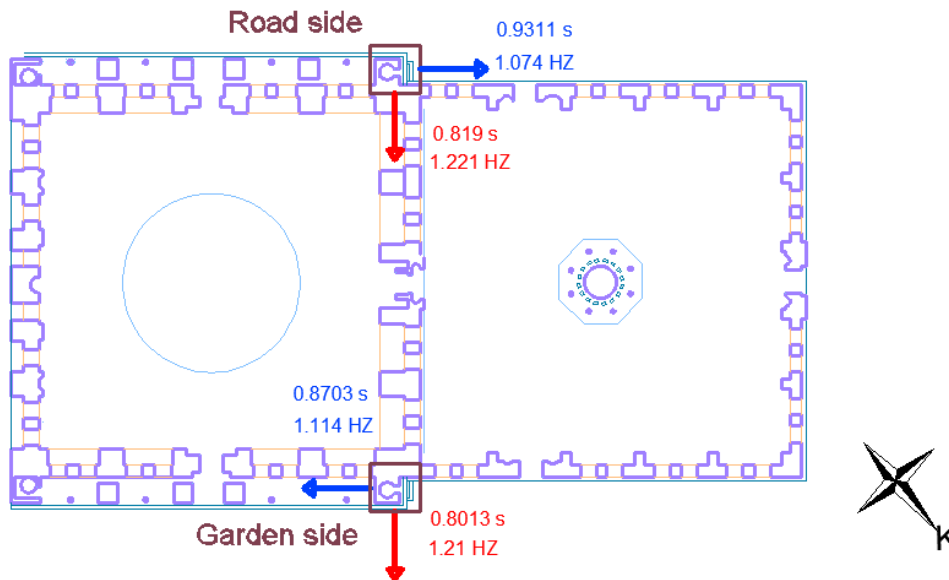


Figure 3.20. 1st mode frequency measured by accelerometers installed at minarets

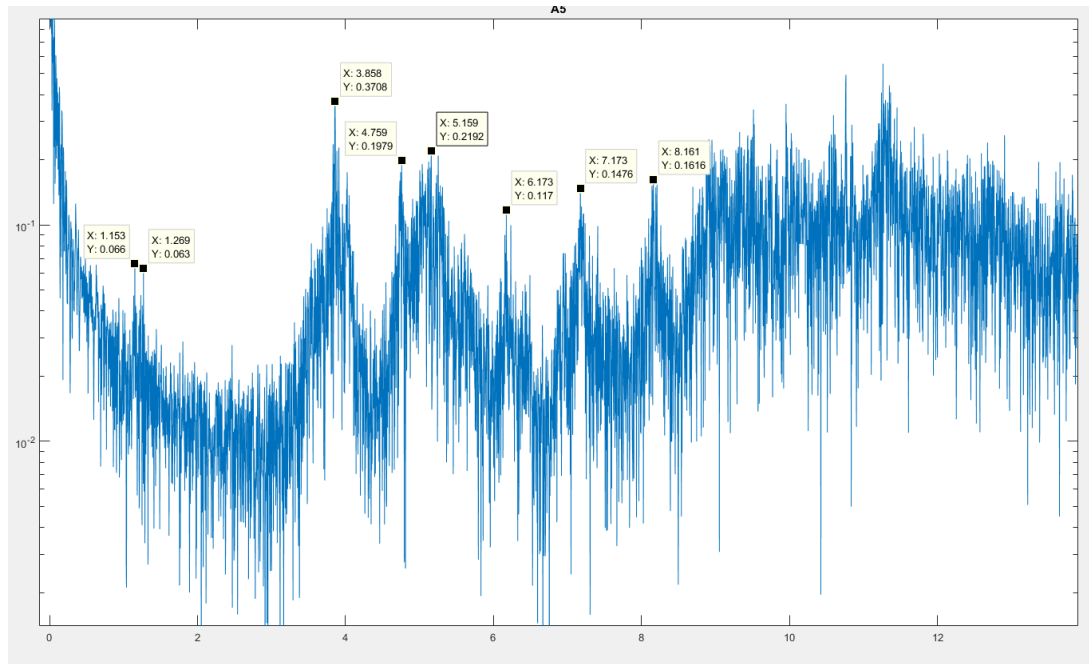


Figure 3.21. Ambient vibration recorded at the main dome

3.2.3.2. 3D- Shell FEM Analysis

The shell model presented in section 3.2.1 is calibrated based on dynamic test results by changing the modulus of elasticity and density of materials. The used material properties and sections thickness are summarized in Table 3.1. The modulus of elasticity and density of stone masonry walls are relatively small since infill materials are used inside main walls. The typical value of modulus of elasticity of stone masonry ranges between 3 and 27 MPa.

Horizontal and vertical springs are used for defining support conditions. K factors for springs are calculated by the resistance of the tributary area of soil below each support, assuming the allowable bearing capacity of soil is 20000 KN/m³.

The 3D model for Şehzade mosque is linearly analyzed for dead load and dynamic load using Turkish code response spectrum shown in Figure 3.22. For unreinforced masonry structures, a reduction factor of 1 is defined. The dynamic loads are defined in X and Y directions with 30% of additional load in Y and X directions respectively. Before calibration when E is assumed 6000 MPa and material density is 2700 Kg/m³,

the first modal period is 0.65 second. The first six modal shapes after calibration are shown in Figure 3.23 with periods of 0.84, 0.83, 0.80, 0.79, 0.38 and 0.36 second, respectively. First mode's period is 0.84 s with less than 5% of error compared to in-situ measured natural frequencies. The minarets have two independent first and second mode shapes since they are not fully identical. The third mode, 0.80 second (1.27 Hz), is also captured by the dynamic test record as shown in Figure 3.21.

Table 3.1. Material properties after calibration and thickness of sections

	Stone walls	Bricks for domes	Stone of main columns	Courtyard marble columns
Modulus of Elasticity (MPa)	3500	3500	20000	30000
Density (Kg/m ³)	2700	1800	2700	2800
Thickness (m)	0.4 - 3.6	0.5 - 0.8	4.5	0.5

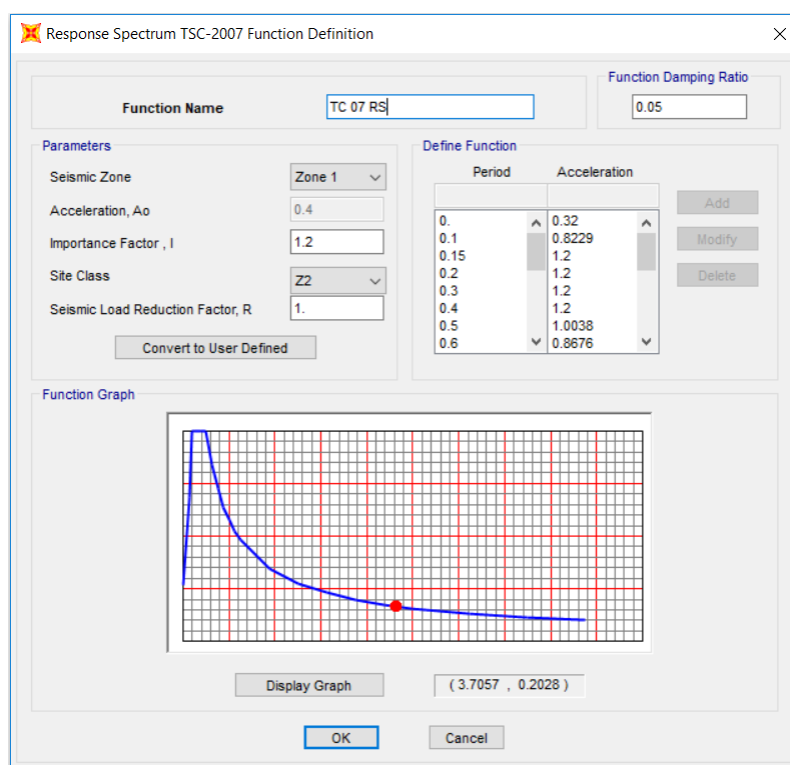


Figure 3.22. Response spectrum function definition using Turkish code

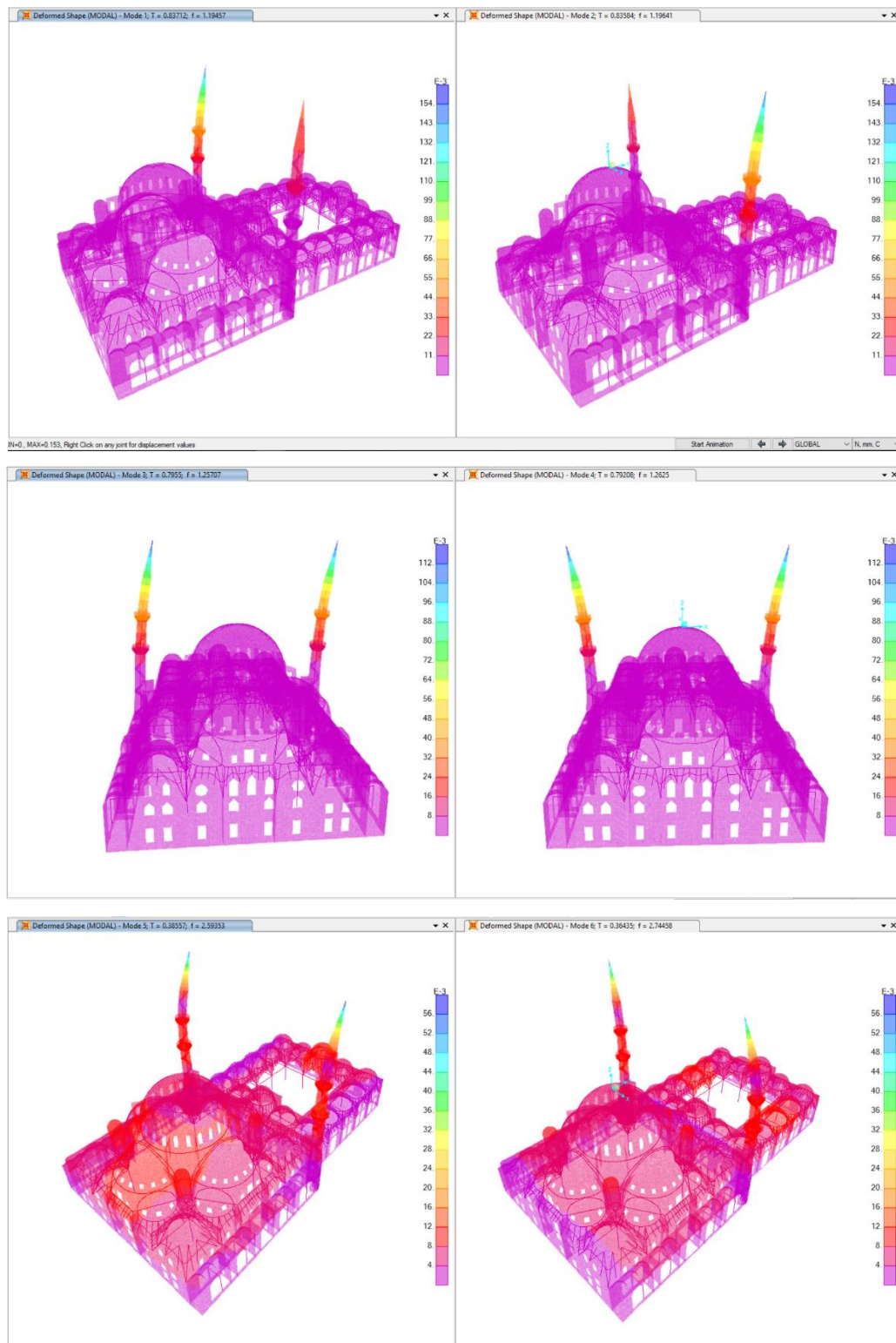


Figure 3.23. First six modal shapes

Staged construction analysis is also performed to consider the sequence of loads applied during construction. Nineteen stages of construction for the mosque are defined as shown Figure 3.24. Figure 3.25 compares between tension stresses S22 from dead and staged dead loads. For top parts of mosque, the stresses are decreased when staged analysis is performed.

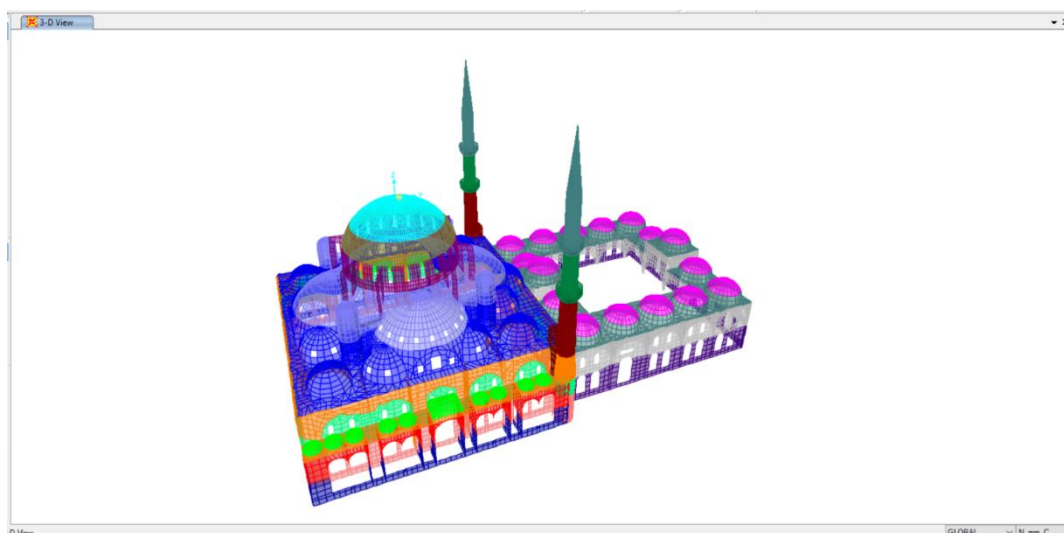


Figure 3.24. Construction stages

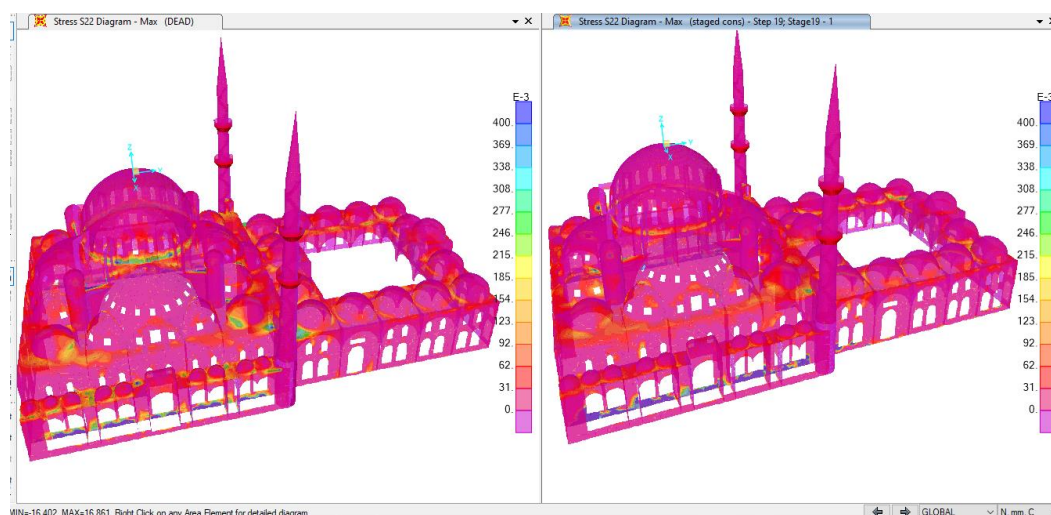


Figure 3.25. Tension stresses S22 from dead and staged dead loads

A comparison between stresses due to static and dynamic loads in both shell and solid model of the mosque are presented in section 3.2.3.4.

3.2.3.3. 3D- Solid FEM Analysis

The modulus of elasticity in Table 3.1 is also defined for the solid elements in 3D solid FE model. The first modal period in the solid model is 0.37 s, when Δ is 0.5m, as shown in Figure 3.26. Since the minarets and side terraces of the mosque are not generated in the solid model due to missing laser scan data for them, the first mode shown in Figure 3.26 corresponds to the fifth mode shape of shell model which has a time period of 0.38 s as shown in Figure 3.27.

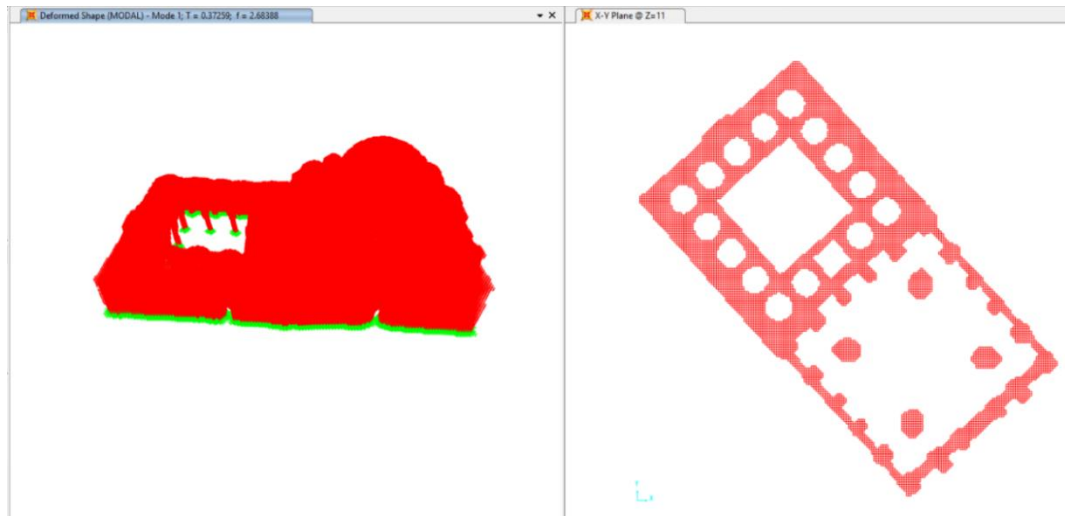


Figure 3.26. First mode of the solid model of the mosque

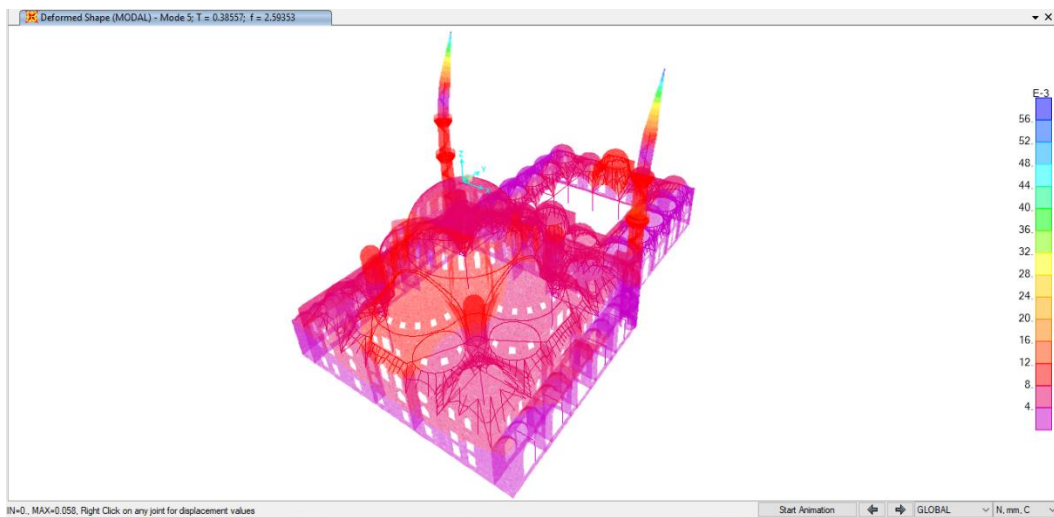


Figure 3.27. Fifth mode shape and period of the shell model

Mesh convergence analysis is performed based on mesh size and analysis results to optimize geometrical and analytical accuracy. As the finite element size get smaller, the analysis becomes more accurate, however, very fine mesh may cause cumulative numerical errors. Coarse mesh gives faster analysis results but affects the analysis reliability. Sensitivity analysis is performed starting from coarse to fine mesh using “i7-7700HQ CPU @ 2.80GHz2801 Mhz, 4 Cores, 8 Logical Processors” computer. The modal period and run analysis time are compared for different mesh size Δ and summarized in Table 3.2. Analysis carried out with a mesh size less than 0.3 m is not complete due to the large number of finite elements. Figure 3.28 shows the geometrical accuracy of the solid model with different mesh size.

Table 3.2. Comparison between solid models of Şehzade mosque with different mesh size

Mesh size Δ (m)	0.5	0.4	0.3	0.2
No. of solids	193456	346443	762243	2117835
No. of nodes	256691	441600	930747	2460834
Generation time (min)	3	6	13	50
Run time	17 min.	3 hours	9 hours	Not run
Modal period (s)	0.372	0.336	0.324	Not run
Mass (ton)	58466	54040	49971	Not run

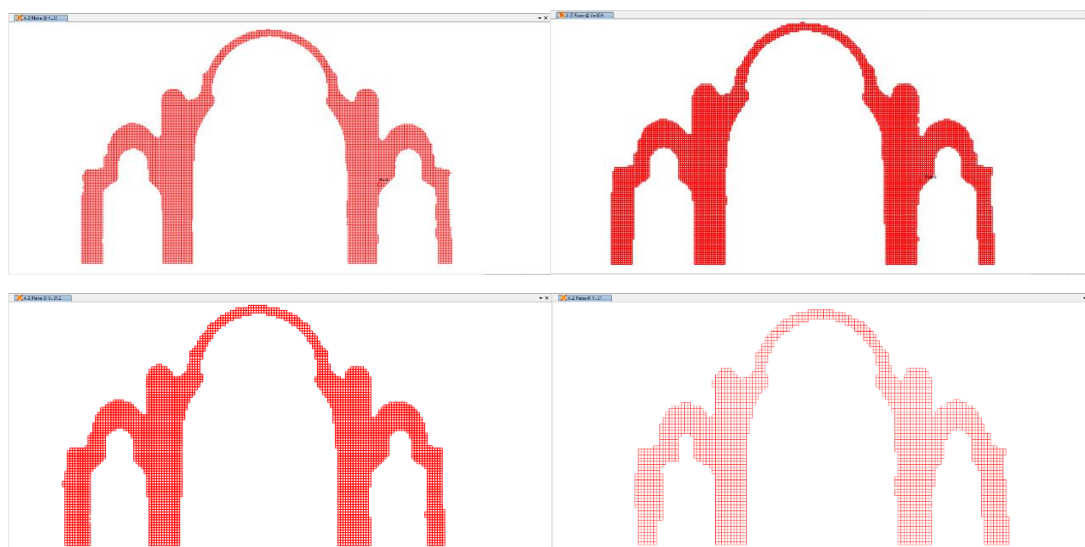


Figure 3.28. A vertical section in solid models with 0.2, 0.3, 0.4, 0.5 m mesh size

3.2.3.4. Comparison Between Shell and Solid FEM Analysis Results

A Comparison of tension and compression stresses of the 3D solid and 3D shell based analytical models for Şehzade mosque is carried out in this section. Table 3.3 summarizes the differences between shell and solid of Şehzade mosque in terms of geometrical accuracy and generation and analysis time. The shell model has about 25% less mass compared to the fine meshed solid models since the corners and pendentives were not properly modelled in the shell model.

Table 3.3. Comparison between 3D shell and solid models for Şehzade mosque

	3D Shell Model	3D Solid Model
Generation Time	2-3 weeks for shell members modeling and meshing	1 day for laser scanning. 1-2 days for point cloud pre-processing ... min. for generation ..min. import to FE program
Run Analysis Time	9 min.	17minutes - 9 hours.
Geometrical Accuracy	Approximated with several assumptions	Accurate geometry

In the 3D shell model of Şehzade mosque, the tension and compression stresses caused by gravity loads are small, less than 200 KPa in tension and 1 MPa in compression as shown in Figure 3.29. Tension and compression stresses due to gravity and earthquake loads in shell and solid ($\Delta = 0.4\text{m}$) FE models are shown in Figures 3.30, 3.31, 3.32, and 3.33, respectively (minarets and side terraces are removed from shell model). It is clear that the tension and compression stresses in the solid model are less than the stresses obtained with shell based analytical model since the geometry in the generated solid model is not distorted at the wall to dome or slab connections and pendentives.

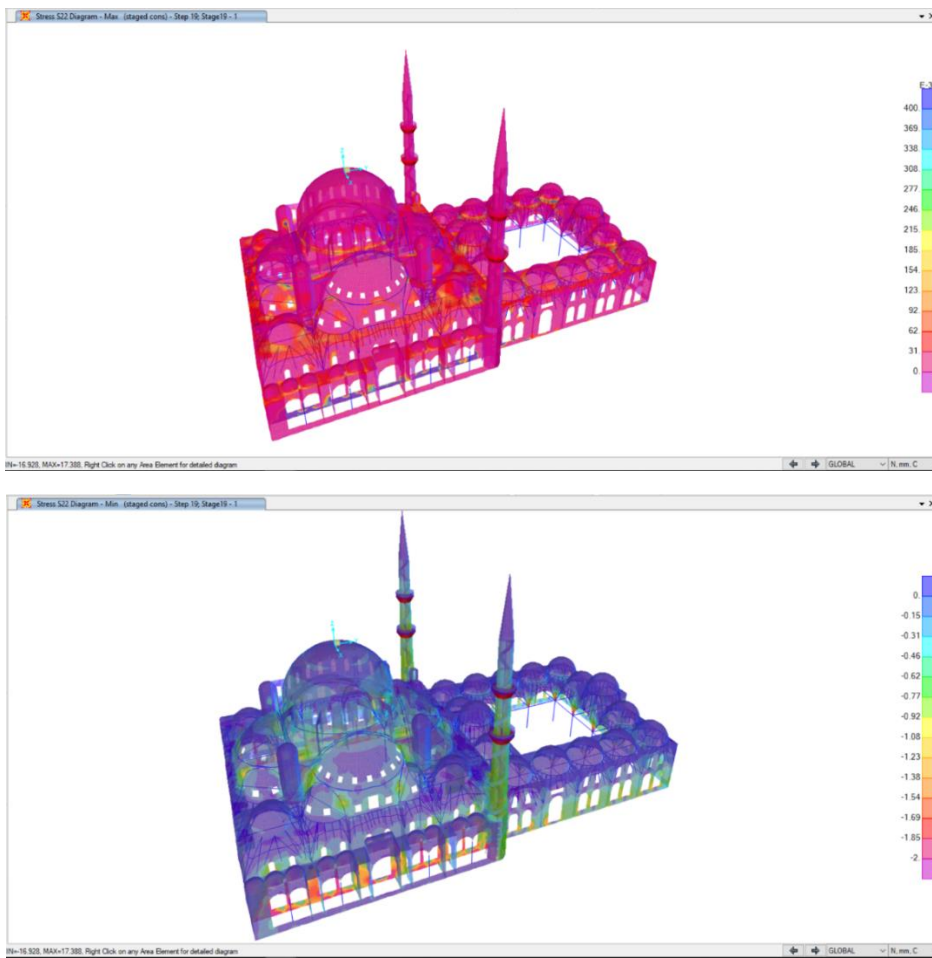


Figure 3.29. Gravity loads tension and compression stresses in the shell model

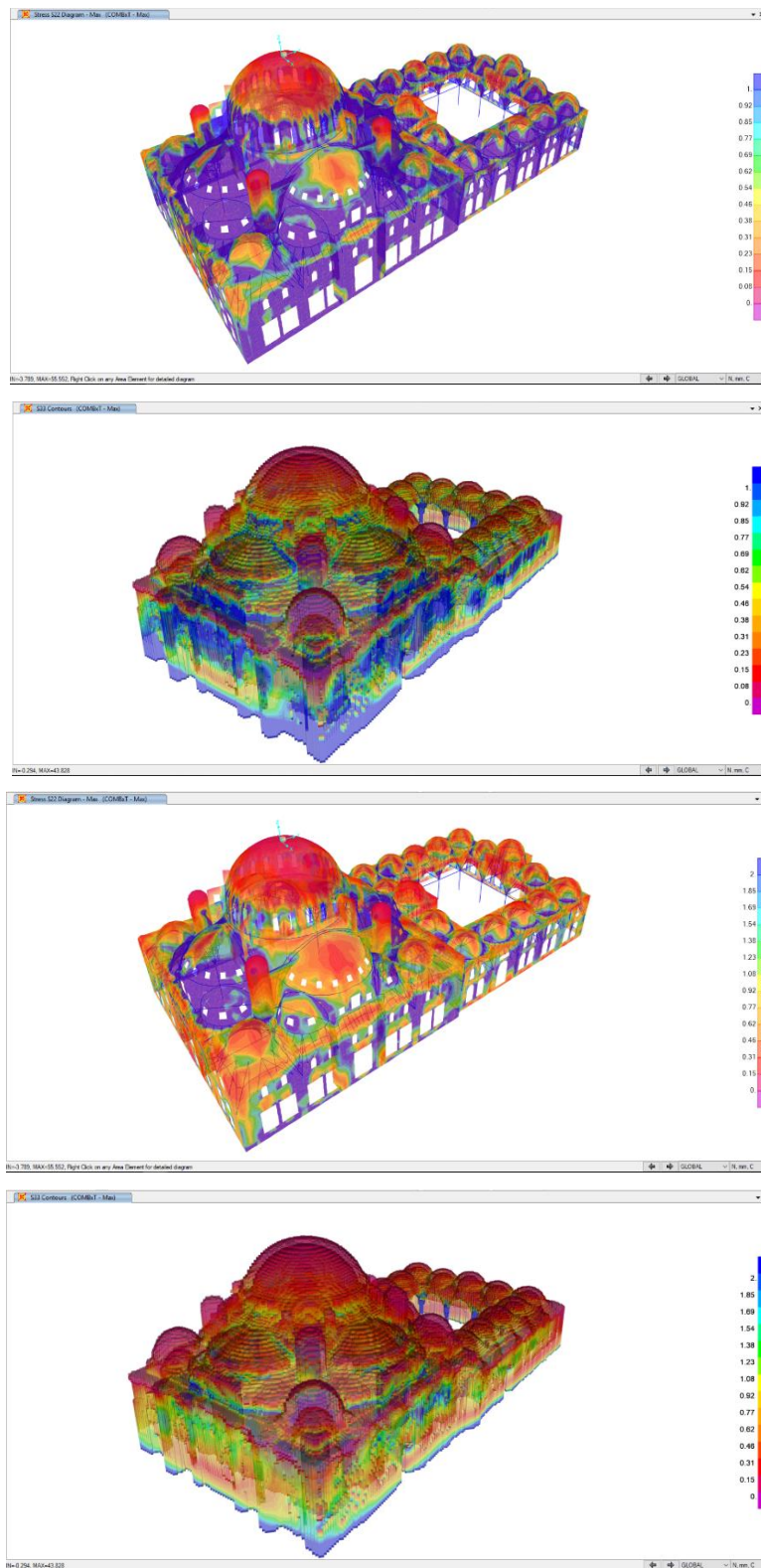


Figure 3.30. Tension stresses from DL and X-direction EQ for both models (0 - 1 MPa & 0 - 2 MPa)

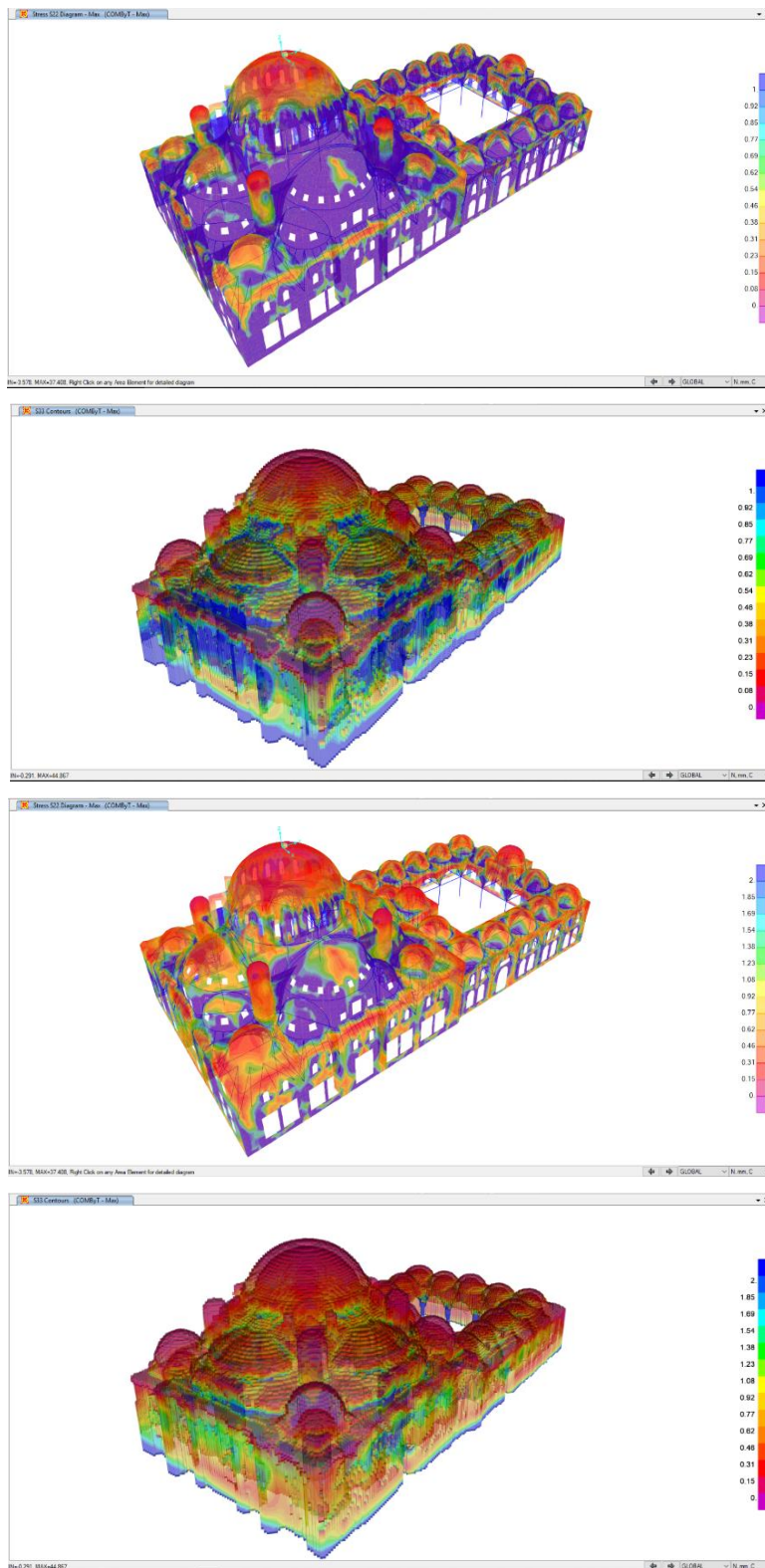


Figure 3.31. Tension stresses from DL and Y-direction EQ for both models (0 - 1 MPa & 0 - 2 MPa)

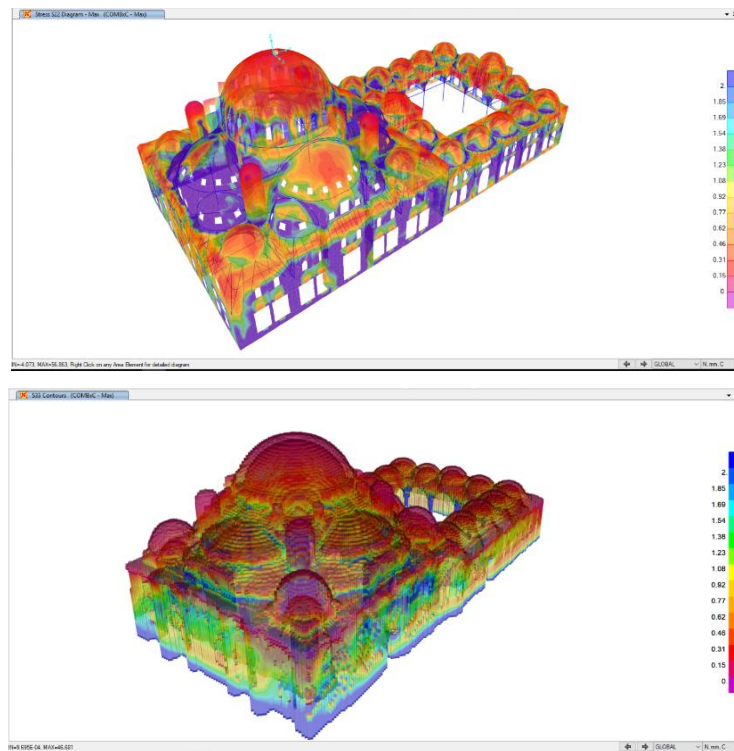


Figure 3.32. Compression stresses from DL and X-direction EQ for both models (0 - 2 MPa)

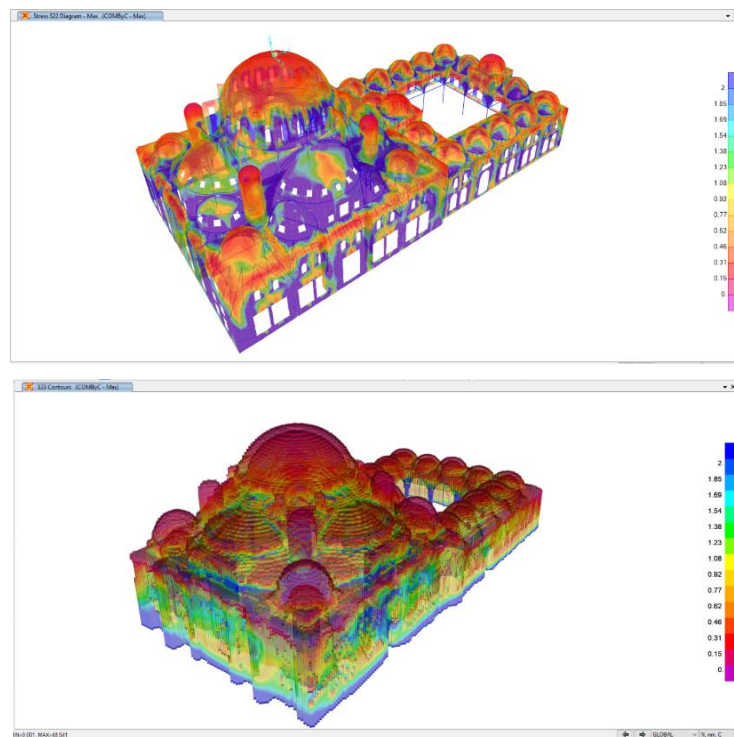


Figure 3.33. Compression stresses from DL and Y-direction EQ for both models (0 - 2 MPa)

Summary for principle stresses compared with limits:

According to previous studies and based on material test, tension limit is assumed to be 0.5 MPa, and compression limit is 4 MPa. Maximum stresses, principle stresses σ_1 σ_2 , are calculated using Mohr circle and compared according to Coulomb-Mohr theory shown in Figure 3.34.

In order to estimate the percentage of safe and unsafe elements in 3D shell and solid models of Şehzade mosque, the following conditions are used to find the ratio between principle stresses and limits:

- 1) If $\sigma_1 > 0$ and $\sigma_2 > 0$ then calculate $\sigma_1/0.5$
- 2) If $\sigma_1 < 0$ and $\sigma_2 < 0$ then calculate $\sigma_2/-4$
- 3) If $\sigma_1 \geq 0$ and $\sigma_2 \leq 0$
if $\sigma_1 = 0$ then calculate $\sigma_2/-4$
else calculate $\sigma_1/-4 \times (-4/0.5 - \sigma_2/\sigma_1)$

The tension and compression principle stresses due to gravity and earthquake loads in Y direction on bottom and top surfaces of shell elements and for solid elements are plotted in Figure 3.35 and Figure 3.36 against the stress limits of Figure 3.34. Moreover, the number and percentage of save and unsafe shell and solid elements are calculated and summarized in Table 3.4 where the principle stresses are compared to two sets of tension and compression limits, 0.5 and 0.8 MPa for tension and 4 and 8 MPa for compression. Total number of shell elements is 70566 while solid elements number is 1048575. This explains the wider distribution of solid elements shown in Figure 3.36 compared to the distribution of shell elements in Figure 3.35.

More than 70% for 0.8 MPa in tension and 8 MPa in compression of shell elements' principle stresses exceeded limits on the inner (bottom) and outer (top) surfaces of shell elements subjected to dead and y-direction earthquake forces. However, only 45% of solid elements' principle stresses exceeded 0.8 MPa tension and 8 MPa compression limits.

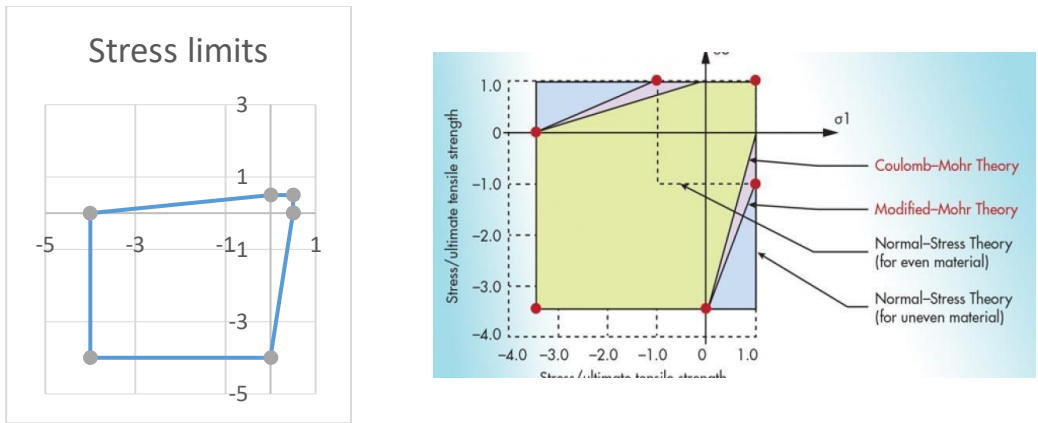


Figure 3.34. Limits of principle stresses using Coulomb-Mohr Theory



Figure 3.35. Principle stresses for shell elements compared to limits

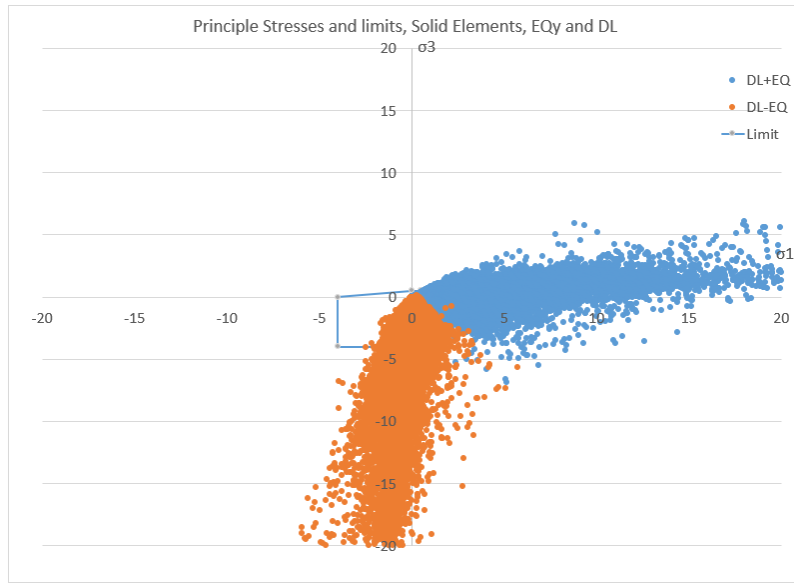


Figure 3.36. Principle stresses for solid elements compared to limits

Table 3.4. Number and percentage of safe and unsafe shell and solid elements of Şehzade mosque FE models

	No. of safe elements	No. of unsafe elements	Safety percentage	Unsafety percentage
Limit: 0.5, 4 MPa				
Shell model (Y direction)	9279	61376	13%	87%
Solid model (Y direction)	262135	786440	25%	75%
Limit: 0.8, 8 MPa				
Shell model (Y direction)	15506	55149	22%	78%
Solid model (Y direction)	570862	477713	55 %	45%

CHAPTER 4

CONCLUSIONS AND FUTRUE WORK

The available procedures for 3D modeling of monumental historical structures based on survey drawings or point clouds are time consuming and labor-intensive approaches. A new innovative 3D solid FE model generator for historical structures with complex geometry using laser scan data is developed and discussed in this thesis. The relevant algorithm developed in this thesis is implemented in three steps: i) defining boundary solids by allocating scan data to corresponding solids, ii) a recursive function is used to navigate into a virtual solid network to recognize the internal solids represent the structural elements, and iii) finally, all boundary and internal finite elements are generated. The proposed procedure is validated to build volumetric finite element models using the point clouds of two pilot study of complex structures. A comparison between the analysis results of shell and solid models is also discussed for a historic mosque.

The algorithm and MATLAB based software worked successfully for both of the pilot test structures using their laser scan data. Comparison of the 3D solid and 3D shell based analytical models for Sehzade Mosque showed that 3D solid model was more successful in determining critical stresses since the geometry is not distorted at the wall to dome or slab connections and filled pendentives at corners. The study results indicate that the developed algorithm is practical to generate solid models from laser scan data; however, quality and density of laser scan data are important for successful model generation. An effective methodology for laser scan data pre-processing is also suggested in this research.

More than 70% for 0.8 MPa in tension and 8 MPa in compression of shell elements' principle stresses exceeded limits on the inner (bottom) and outer (top) surfaces of

shell elements subjected to dead and y-direction earthquake forces. However, only 45% of solid elements' principle stresses exceeded 0.8 MPa tension and 8 MPa compression limits. Time history analyses are also performed and yielded similar results when compared to response spectrum analysis (see Appendix).

Although shell model gave relatively higher stresses, the mass comparison showed that shell model has about 25% less mass compared to the fine meshed solid model since the corners and pendentives were not properly modelled in the shell model. Therefore, the shell model was deemed to be too conservative and not fully appropriate for modeling of historic massive structures with complex geometry. Although solid members are simple, they can much better simulate the geometry and now easier to generate using the algorithm and software developed in this thesis.

For future work, a Ground Penetration Radar test can be used to detect any possible cavitation or voids inside historical masonry structures to better simulate the geometry and material properties of the scanned structures, thus both linear and nonlinear analysis can be conducted.

A user-friendly interface for the 3D solid FEM generator can be developed. The size of solid finite element can be optimized based on the complexity of structure and time and convergence of analysis. Also, a smoothing algorithm can be applied to increase geometrical accuracy.

REFERENCES

Almac, U., Pekmezci, I.P. and Ahunbay, M. 2016. Numerical Analysis of Historic Structural Elements Using 3D Point Cloud Data. *The Open Construction and Building Technology Journal*, 10.

Arias, P., Armesto, J., Di-Capua, D., González-Drigo, R., Lorenzo, H. and Perez-Gracia, V. 2007. Digital photogrammetry, GPR and computational analysis of structural damages in a mediaeval bridge. *Engineering Failure Analysis*, 14, 1444-1457.

Barrile, V., Bilotta, G., D'amore, E., Marando, R., Meduri, G.M. and Trovato, S. 2015. Structural Analysis of Cultural Heritage assisted by 3D Photogrammetry. *Advances in Environmental and Geological Science and Engineering Book*, Salerno, Italy, 193-198.

Bitelli, G., Castellazzi, G., D'Altri, A.M., De Miranda, S., Lambertini, A. and Selvaggi, I. 2016. AUTOMATED VOXEL MODEL FROM POINT CLOUDS FOR STRUCTURAL ANALYSIS OF CULTURAL HERITAGE. *International Archives of the Photogrammetry, Remote Sensing & Spatial Information Sciences*, 41.

Castellazzi, G., D'Altri, A.M., Bitelli, G., Selvaggi, I. and Lambertini, A. 2015. From laser scanning to finite element analysis of complex buildings by using a semi-automatic procedure. *Sensors*, 15, 18360-18380.

Ercan, T. and Çaktı, E. 2017. USE OF LASER SCANNING IN CIVIL AND EARTHQUAKE ENGINEERING.

Hayes, C., and Richie, E. 2015. When to Use Laser Scanning in Building Construction: A Guide for General Contractors, United States.

Hinks, T., Carr, H., Truong-Hong, L. and Laefer, D.F. 2012. Point cloud data conversion into solid models via point-based voxelization. *Journal of Surveying Engineering*, 139, 72-83.

Huber, D., Akinci, B., Oliver, A.A., Anil, E., Okorn, B.E. and Xiong, X. 2011. Methods for automatically modeling and representing as-built building information models. In *Proceedings of the NSF CMMI Research Innovation Conference*.

Kaszynski, A.A., Beck, J.A. and Brown, J.M. 2018. Automated Meshing Algorithm for Generating As-Manufactured Finite Element Models Directly from As-Measured Fan Blades and Integrally Bladed Disks. In *ASME Turbo Expo 2018: Turbomachinery Technical Conference and Exposition*. American Society of Mechanical Engineers, V07CT35A024-V07CT35A024.

Korumaz, M., Betti, M., Conti, A., Tucci, G., Bartoli, G., Bonora, V., Korumaz, A.G. and Fiorini, L. 2017. An integrated Terrestrial Laser Scanner (TLS), Deviation Analysis (DA) and Finite Element (FE) approach for health assessment of historical structures. A minaret case study. *Engineering Structures*, 153, 224-238.

Lubowiecka, I., Armesto, J., Arias, P. and Lorenzo, H. 2009. Historic bridge modelling using laser scanning, ground penetrating radar and finite element methods in the context of structural dynamics. *Engineering Structures*, 31, 2667-2676.

Pauly, M., Mitra, N.J. and Guibas, L.J. 2004. Uncertainty and variability in point cloud surface data. *SPBG*, 4, 77-84.

Taubin, G. 1995. Curve and surface smoothing without shrinkage. *Fifth International Conference. IEEE*, 852-857.

Theiler, P.W. and Schindler, K. 2012. Automatic registration of terrestrial laser scanner point clouds using natural planar surfaces. *ISPRS Annals of Photogrammetry, Remote Sensing and Spatial Information Sciences*, 3, 173-178.

APPENDIX

Time History Analysis

The 3D model of Şehzade mosque is also analyzed using time history analysis with El-Centro, Kobe and Northridge earthquake records which have peak accelerations of 0.3g, 0.8g and 0.8g respectively. Figure A.1 and Figure A.2 show the comparison of tension and compression stresses when TH and RS analysis methods are applied, RHS is the RS result and LHS is the TH result. A slight difference is noticed in stresses results when RS and TH are applied.

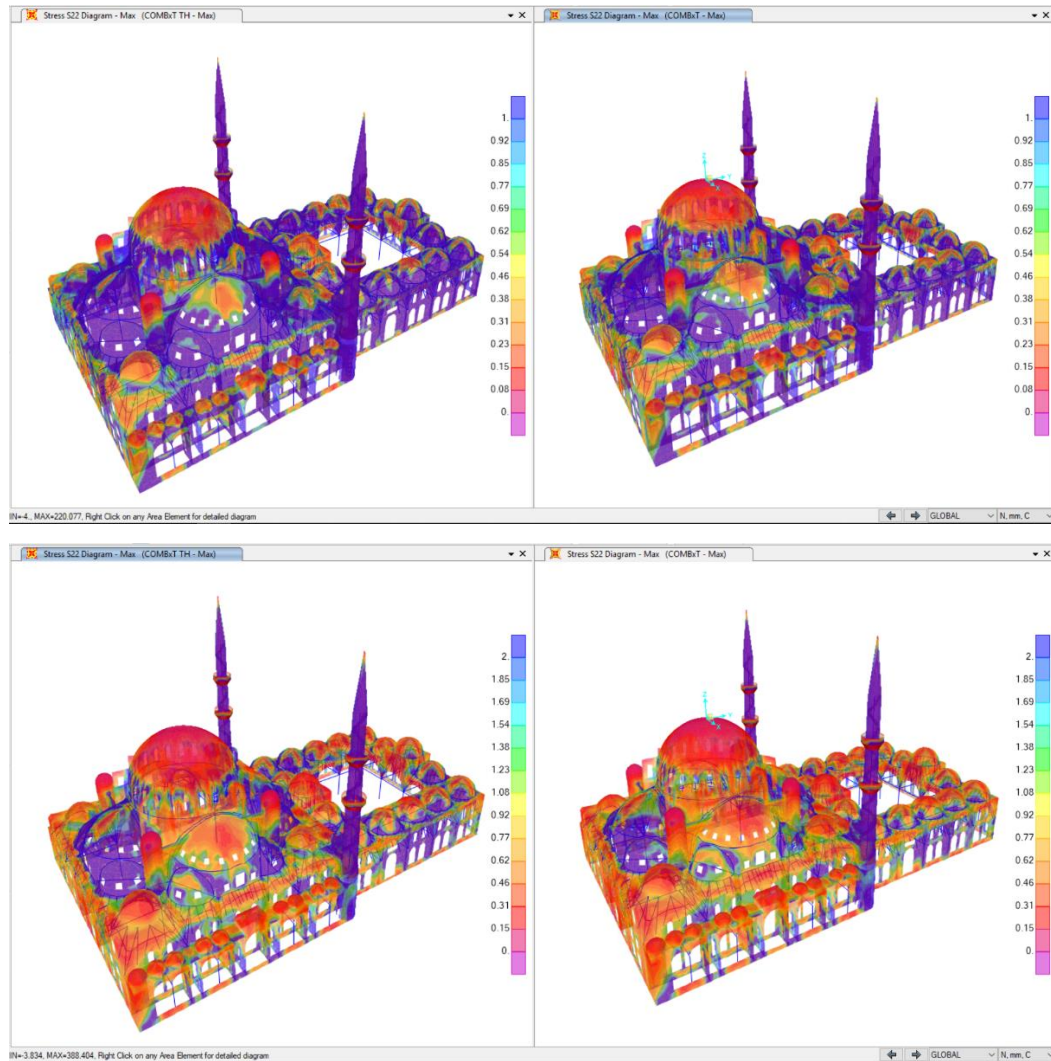


Figure A.1. Tension stresses from dead load and TH load in X-direction (0 - 1 & 0 - 2 MPa)

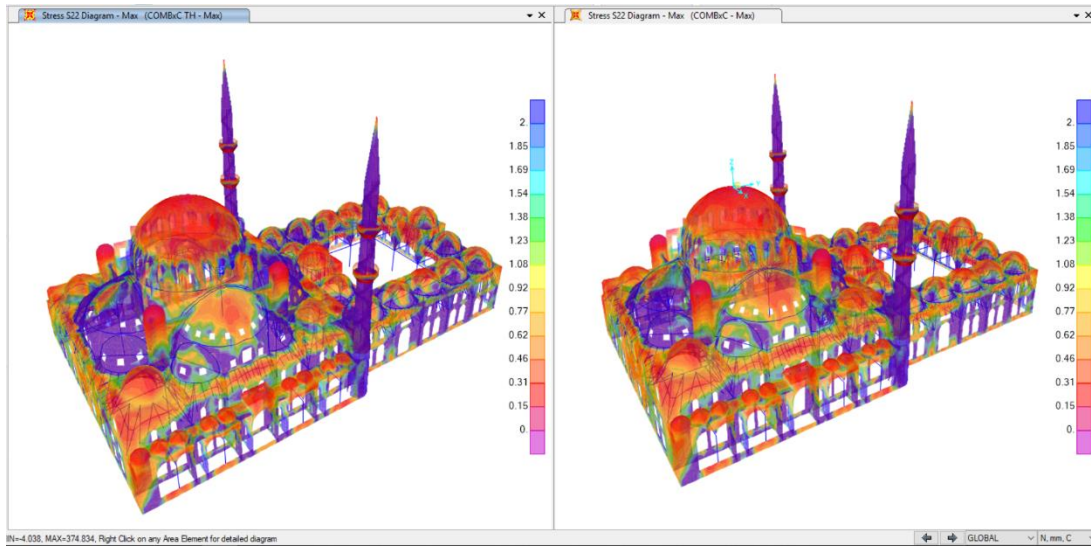


Figure A.2. Compression stresses from dead load and TH load in X-direction (0 - 2 MPa)